pharmaceutics

MDPI

Review

Fluorescent nanosystems for drug tracking and theranostics: recent applications in the ocular field

Elide Zingale [1§], Alessia Romeo [1§], Salvatore Rizzo [1], Cinzia Cimino [1], Angela Bonaccorso [1, 2], Claudia Carbone [1,2], Teresa Musumeci [1,2] and Rosario Pignatello [1,2] *

[1] Department of Pharmaceutical and Health Sciences, University of Catania, Italy;
[2] NANO-i – Research Center for Ocular Nanotechnology, University of Catania, Catania, Italy;
* Correspondence: rosario.pignatello@unict.it

[§] These Authors equally contributed to the work.

Abstract:

The greatest challenge associated with topical drug delivery for the treatment of diseases affecting the posterior segment of the eye is to overcome the poor bioavailability of the carried molecules. Nanomedicine offers the possibility to overcome the obstacles related to physiological mechanisms and ocular barriers by exploiting different ocular routes. Functionalization of nanosystems by fluorescent probes could be a useful strategy to understand the pathway taken by nanocarriers into the ocular globe and to improve the desired targeting accuracy. The application of fluorescence to decorate nanocarrier surface or the encapsulation of fluorophore molecules makes the nanosystems a light probe useful in the landscape of diagnostics and theranostics.

In this review a state of the art on ocular routes of administration is reported, with a focus on pathways undertaken after topical application. The review is divided into three sections involving fluorescent nanosystems for ocular delivery. The first section presents fluorescent nanocarriers used for tracking cellular internalization and permeation of ocular tissues; the systems are discussed classifying them according to their nature (lipid-based, polymer-based, metallic-based and protein-based). The following sections are dedicated to diagnostics and theranostics uses, respectively, which represent an innovation in the ocular field obtained by combining dual goals in a single administration system.

Citation: Lastname, F.; Lastname, F.; Lastname, F. Title. *Pharmaceutics* **2022**, *14*, x. https://doi.org/10.3390/xxxxx

Academic Editor: Firstname Lastname

Received: date
Accepted: date
Published: date

Keywords: nanotechnology; fluorescence; ocular delivery; probes; diagnostics; PKs.

1. Introduction

In recent years, vision-related problems have acquired a greater relevance, due to the ageing of world's population that leads to an increase in visual problems, such as cataract, glaucoma, age-related macular degeneration and diabetic retinopathy, which occur more frequently in over-60s [1,2]. Many visual diseases are associated with neurodegenerative disorders [3,4]. Young people over the age of 18 also suffer from visual problems, which increase especially with the growing use of electronic devices [5]. The raising number of people with vision impairment leads to a greater interest in dedicated care and treatments. This situation increases the costs in the global economy destined to the care of these disorders [6]. In addition, ocular therapy is a serious challenge because of the difficulty in targeting a drug to the appropriate ocular tissues.

In this landscape, technological research is actively involved, with the aim of developing innovative systems for targeted drug delivery [7]. The eye is a very complex structure, both anatomically and physiologically, and the treatment of pathologies affecting this organ is therefore not simple [8-10]. This is related to the various aspects that limit the transportation of drugs to the target site: anatomical barriers, physiological processes, mechanisms and metabolic aspects [11,12]. Reaching the target becomes more complicated if therapy is addressed to the posterior segment of the eye [13-16]. For this purpose, the major administration route remains intravitreal injection, which is invasive and produces undesirable effects as pain and discomfort, inducing patient noncompliance [17,18]. The preferred route of administration would undoubtedly be the topical one, but conventionally it is used to treat diseases of the anterior eye. In fact, it is estimated that only a very small percentage of the drug instilled to the eye surface reaches the anterior chamber (around 5%) and even less the posterior segment [19-21].

To overcome these issues, nanotechnology represent a field of recent interest. One potential strategy for improving drug delivery to the different eye tissues uses nanocarriers with specific size and surface properties, designed to ensure successful achievement of the drug to the target tissue, as well as the potential for a controlled release of the loaded drug, reducing the frequency of treatment and improving the retention time on the corneal surface [22-24]. Currently, the most widely studied nanosystems are used in the treatment of anterior eye diseases such as cataracts [25], glaucoma [26], dry eye syndrome [27], keratitis [28], conjunctivitis [29], uveitis [30], but also posterior eye diseases such as retinitis [31], macular degeneration [32], endophthalmitis [33] and ocular tumours [34].

Suitable drug nanocarriers possess a mean size in the nanometric range and are classified according to their structural composition and the materials used, that must be biodegradable and biocompatible [35]. Many reviews focus on the development of nanosystems designed for ocular delivery, but none on the ophthalmic use of fluorescent nanocarriers. It is not certain that after their administration the drug effectively reaches the target site; therefore, during its design, tracking studies are necessary to demonstrate its distribution and positioning.

One possible strategy is to follow the nanosystem movements using a fluorescent probe. Fluorescence is a simple and non-invasive way to track the drug through the eye tissues, and it is also widely used in diagnostics to visualize diseased tissues, lesions and pathological markers. The development of personalized medicine and need for early intervention in the diagnosis and treatment of specific diseases have promoted the birth and development of a new discipline, theranostics [36]. It can be defined as the combination of diagnostics with a specific therapeutic treatment. *In vitro* diagnostics and prognostics, *in vivo* molecular imaging, molecular therapeutics, image-guided therapy, biosensors, nanobiosensors and bioelectronics, system biology and translational medicine and point-of-care are some recent application examples.

This review deals with the use of fluorescent probes in the last 5 years applied to nanomedicine in the ophthalmic field. The aim is to illustrate the state-of-the-art on fluorescent nanosystems divided according to their application: fluorescent nanosystems for biodistribution studies to clarify the best performing nanoparticle design and delivery

strategies able to address specific ocular diseases, for diagnostics and finally for the emerging field of theranostics. PubMed database was used to perform an advanced search. The time frame set included the range from January 2017 to February 2022. The keywords used were "fluorescence", "nanoparticles", "ocular" and "delivery", "theranostics", "diagnostics". Articles were limited to "Free full text" and "Full text" articles in English language published in journals with an impactor factor not less than 4. The same process was repeated on ScienceDirect database. Reference lists of articles were also reviewed for additional citations.

2. General aspect of the human eye

The eyeball consists of three chambers: anterior, posterior (containing the aqueous humor) and the vitreous chamber (containing the vitreous body). The wall is composed of three tunics [8,37]. The first, called external, is composed anteriorly of the cornea and for the remaining part of the sclera. The middle tunic (uvea) is richly vascularized and pigmented, and includes the iris, the ciliary body and the choroid. Finally, the internal or nervous tunic is represented by the retina [38]. The sclera is anteriorly lined by the conjunctiva. Its function is to maintain the shape of the bulb and to provide attachment to the tendons of the striated muscles of the eye [39]. The cornea is a transparent lamina without vessels (necessary conditions for the passage of light). Under the cornea there is the iris, a sphincter of pigmented smooth muscle that regulates pupillary caliber. Trophism in this district is provided by the aqueous humor [40]. The ciliary body is an ocular anatomical structure responsible for both the production of aqueous humor and the control of accommodation. The ciliary body is located immediately posterior to the iris and anterior to the choroid. Posterior to the iris and in front of the vitreous body the crystalline is situated, which transmits and focuses light onto the retina. It consists of a single layer of epithelial cells that, during fetal development, migrate laterally toward the equator of the lens where it inverts, elongates, synthesizes large amounts of specific proteins, and finally degrades organelles so as to increase transparency [20]. From a physiological perspective, there are two reflexes involved in vision: lens accommodation (regulates convexity) and pupillary reflex (regulates pupil caliber). The accommodation allows the focal point to fall always at the level of the retina, allowing both short and long-distance vision. Furthermore, the pupillary reflex regulates the intensity of incoming light. Finally, the transduction of light impulses at the retinal level into visual images is mediated by photoreceptors which generate nerve stimuli that reach the contralateral posterior cortex through the optic nerve [41-43]. The delivery of a drug into the eye tissues is related to two different routes of administration, that are divided into invasive and non-invasive routes. A list of these routes is showed in the Table 1.

Table 1. Conventional route of ocular delivery: benefits and limits. 134

ADMINISTRATION ROUTE	BENEFITS	LIMITS	OCULAR ANTERIOR / POSTERIOR TARGET	References
Oral	• Non-invasive. • Increased compliance.	• Difficult achievement of the anterior and posterior tracts of the eye. • Possible degradation by digestive fluids. • Possible low absorption and bioavailability. • Hepatic first-pass metabolism. • Presence of anatomical barriers (blood-aqueous barrier and the blood-retinal barrier).	Potentially both	[44-47]
Systemic	• Avoided first-pass metabolism.	• Difficult achievement of the anterior or posterior segment of the eye. • Lower compliance. • Presence of anatomical barriers (blood-aqueous barrier and the blood-retinal barrier).	Potentially both	[47,48]
Parenteral (intravitreal, subretinal, suprachoroidal, subconjunctival, intracameral, intrascleral, and intrastromal)	• Deposit of the therapeutic agent in the eye, in some cases directly at the site of action. • Increased local concentration of the drug. • Reduced required dose and avoided off-target actions. • Bypassing of ocular epithelium and other barriers, resulting in increased bioavailability.	• Administration performed by specialized personnel. • Invasive technique. • Short-term complications, including retinal damage, endophthalmitis, haemorrhage, intraocular inflammation, and increased Intraocular Pressure (IOP).	Posterior	[49-54]
Topical	• Over 90% of the ophthalmic product on the market.	• Rapid precorneal elimination of the drug due to eyelid reflex, tear drainage, dilution by tears, and systemic absorption from the conjunctival sac. • Misapplication of the product to the ocular surface. • Presence of corneal epithelial barrier. • Narrow barriers at the front and back of the eye (limit and regulate fluid and solute uptake). • Complex kinetic processes of absorption, distribution and elimination, influenced by physiology, the physicochemical properties of the drug (lipophilicity, charge, size and shape of the molecule) and the formulation (pH, buffer, tonicity, viscosity, possible presence of preservatives and stabilizers). • Allowed permeation of small lipophilic molecules through the cornea and of larger or hydrophilic compounds through the conjunctiva and the sclera. • Achievement f the anterior segment for only 1% of the administered dose segment, and an even smaller percentage to the posterior segment.	Both	[55-63]

The corneal epithelium and endothelium (lipophilic in nature) consist of cells connected by tight junctions that limit the passage of large molecules. The hydrophilic stroma consists of tightly packed collagen. The epithelium, however, provides the greatest resistance to diffusion. The paracellular pathway through the intercellular pores is allowed for small ionic and hydrophilic molecules of size < 350 Da, whereas the transcellular pathway allows passage of larger lipophilic molecules. The variations in lipophilicity of the corneal layers allowed the realization of a parabolic relationship between corneal permeability and diffusion coefficient. pH is another important factor in corneal permeability [37]. Many studies that have examined permeability across conjunctiva, tenon, and sclera have shown that the conjunctiva is more permeable to hydrophilic molecules than the cornea. The greater surface area (in humans about 17 times bigger than the cornea) and the presence of larger pore sizes promote increased permeability compared to the cornea. However, mucus and the presence of lymphatics and vasculature increases systemic leakage [24,37]. In ocular topical administration, reaching the posterior portion is size-dependent [64]. Nanocarriers with a diameter of 20-200 nm are suitable for retinal-targeted delivery. Small nanoparticles (20 nm) are able to cross the sclera and are rapidly eliminated due to periocular circulation. The larger ones (200 nm) do not cross the sclera or the sclera-choroid-retinal pigment epithelium (RPE) and remain in the periocular site releasing their contents even for long periods. Even in the case of intravitreal administration, the kinetics are size-dependent. Nanocarriers with a diameter of 2 mμ remain in the vitreous cavity or migrate into the trabeculae. Those with a diameter of less than 200 nm reach the retina [65]. In order to discuss the application of nanosystems in ocular field, an emergent role is represented by fluorescent nanosystems. The tailor ability of design, architecture, and photophysical properties has attracted the attention of many research groups, resulting in numerous reports related to novel nanosensors to analyze a great variety of biological analytes.

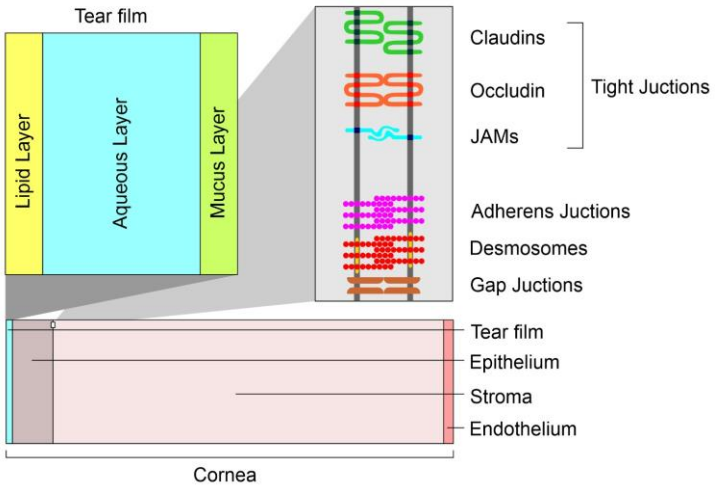

Figure 1. Cross-section of corneal tissues: barriers to drug penetration after topical instillation.

3. Fluorescent probes in ocular applications

Before focusing on the published experimental studies, in this section a brief discussion on fluorescence and on the molecules applied in the ocular field is given.

Absorption of a photon from a fluorescent chemical species causes a transition to an excited state of the same multiplicity (spin) as the fundamental state (S_0). In solution, S_n states (with $n > 1$) rapidly relax to S_1 through nonradiative processes. Ultimately, relaxa-

tion from S_1 to S_0 causes the emission of a photon with an energy lower than the absorbed photon. The fluorescence quantum yield (φ), one of the most important parameters, provides the efficiency of the fluorescence process; it is defined as the ratio between the number of photons emitted to those absorbed.

$$\varphi = \frac{Number\ of\ photons\ emitted}{Number\ of\ photons\ absorbed}$$

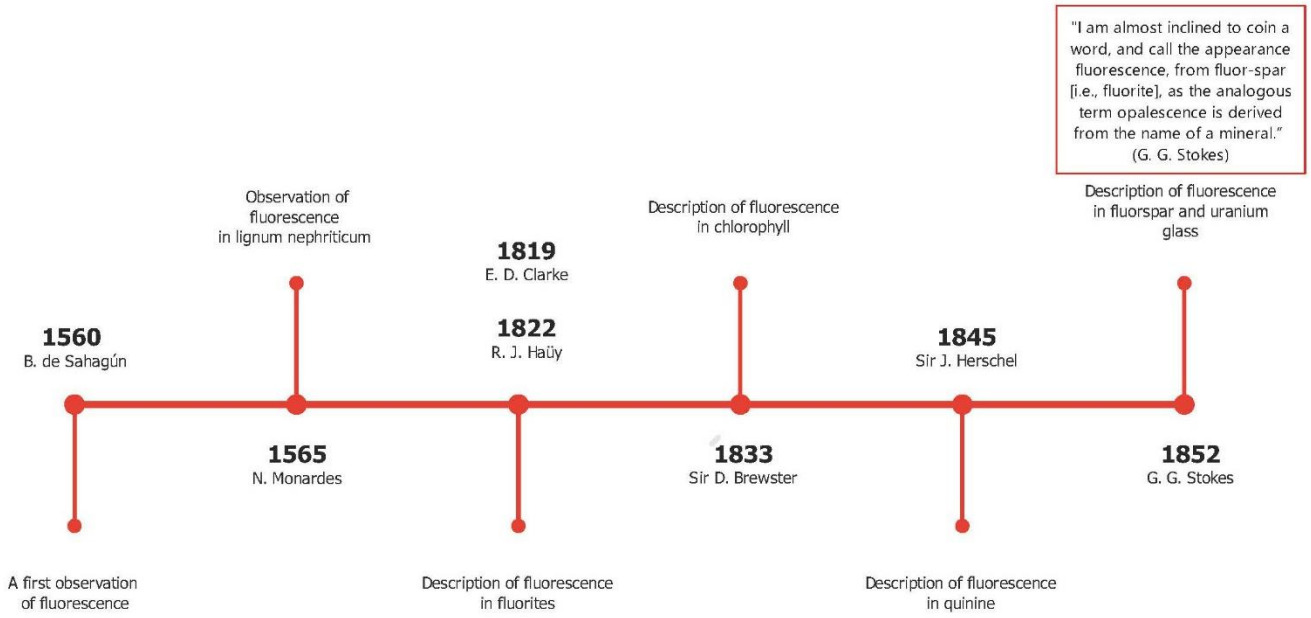

Figure 2. Timeline of the fluorescence discovery.

In Figure 2, we reproduce a brief history of the discovery of the fluorescence phenomenon. This discovery enabled the development of fluorescent probes that achieve single-molecule sensitivity. The figure shows that the first observation of a fluorescence phenomenon was described in 1560 by Bernardino de Sahagun; the same experiment was repeated by Nicolas Monardes in 1565. The fluorescence of the infusion known as lignum nephriticum was observed. This phenomenon was caused by the fluorescence of the oxidation product of one of the flavonoids present in those woods: matlaline. In the middle of the nineteenth century, George Gabriel Stokes coined the term fluorescence, derived from fluorite. The knowledge of atomic structure needed to understand and describe the nature of the phenomenon was not acquired until the beginning of the 20th century. By providing detailed information, this technique has enormous advantages over classical microscopy techniques [66]. In fact, literature is plentiful of studies dealing with the design of new fluorescent probes such as (bio)sensors to detect (even with the naked eye) enzymes, metals, biomaterials, and others. Since 1945, the ability of analytes to promote the opening of rhodamine spirolactams has been exploited to design probes that detect metal ions and biological targets [67,68]. The pH sensitivity of fluorescein can be used to detect changes in a specific environment. By controlling the balance of ring

opening and closing, following the interaction with specific targets, it can be used to detect metal ions from industrial and commercial specimens [69]. Curcumin is also widely used as a fluorescent probe for different applications, from producing drug carriers to the realization of specific sensors for ions and biomolecules [70,71].

The following section delineates the family of fluorescent probes reported in reviewed studies, while Table 2 gathers the probes that are used in the experimental papers cited in this review.

Table 2. Physico-chemical properties of the main fluorescent probes used in ocular bio-imaging.

PROBE	CHEMICAL STRUCTURE	MOLAR MASS (g mol^{-1})	SOLUBILITY IN WATER	EXCITATION (nm)	FLUORESCENCE (nm)
Coumarin-6	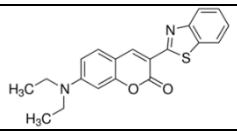	350.43	Insoluble	488-666	502-649
Curcumin	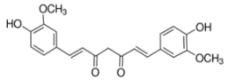	368.38	Insoluble	300-470	571
Cyanine 5-phosphoramidite	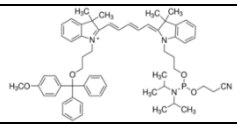	944.21	Insoluble	649	666
1,1′-dioctadecyl-3,3,3′,3′-tetramethylindocarbocyanine perchlorate	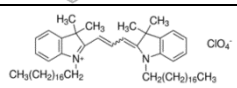	933.87	Low	550	565-588
Fluorescein	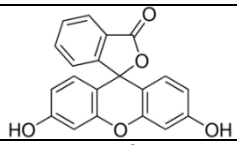	332.31	Insoluble	465-490	494
Fluorescein sodium salt	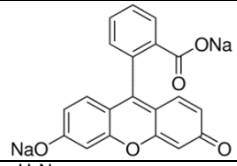	376.27	Soluble	460	512
5-aminofluorescein	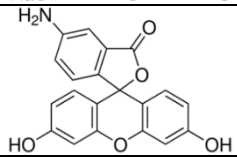	347.32	Soluble	450-490	500-550
Fluorescein-5-isothiocyanate	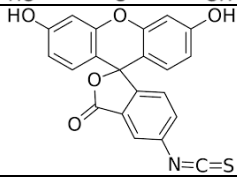	389.38	Insoluble	495	519
5-(iodoacetamido)fluorescein	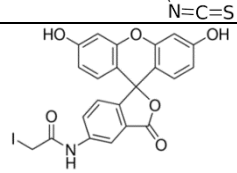	515.25	Insoluble	492	518

5(6)-carboxyfluorescein	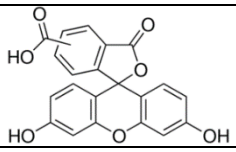	376.32	Low	495	520
Nile Red	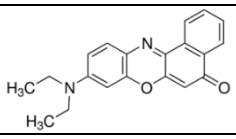	318.37	Insoluble	543-633	550-700
Rhodamine B	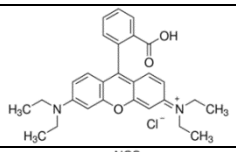	479.01	Soluble	488-530	600-633
Rhodamine B isothiocyanate	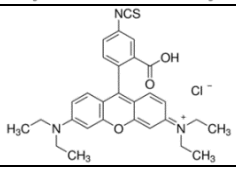	536.08	Insoluble	553	563-650
Rhodamine 123	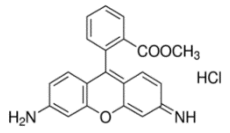	380.82	Low	488	515-575
Rhodamine 6G	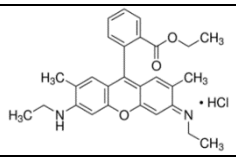	479.01	Soluble	480	530
Toluidine Blue O	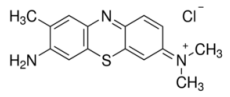	305.83	Soluble	595	626

3.1 The coumarins family

Coumarins have a conjugated double ring system. In industry, coumarins find application as cosmetic ingredients, perfumers, food additives, and in synthetic pharmaceuticals. In nature, coumarins are found in a wide variety of plants: tonka bean (*Dipteryx odorata*), sweet wood (*Galium odoratum*), vanilla grass (*Anthoxanthum odoratum*) and sweet grass (*Hierochloe odorata*) [72]. Among the different synthetic derivatives, Coumarin-6 (C6) exhibits acid-base properties. In the study of Duong et al., a membrane with C6 demonstrated to exhibit colorimetric and ratiometric fluorescence properties with a dynamic pH range between 4.5 and 7.5 (the study uses blue nile in parallel) [73].

3.2 Fluorescein family

Fluorescein is a xanthene dye with yellowish green fluorescence. It was firstly synthesized in 1871 by von Bayer via Friedel's acylation/cyclodegradation reaction using resorcinol and phthalic anhydride [74]. It has a rigid tricyclic-coplanar structure with two aryl groups fused to a pyran ring. It has two distinct structures, an open fluorescent ring in the carboxylic acid form and a closed non-fluorescent ring in the spirocyclic lactone form. The open-closed equilibrium in the structure of fluorescein makes it sensitive to the pH of the medium [75]. Among the amine derivatives of fluorescein, those with one

or two NH_2 groups in the phthalic residue are of particular interest. The corresponding (di)anions do not show intense fluorescence unless the amine groups are involved in new covalent bonds. In alcohols, the quantum yield, φ, is quite low. In dimethylsulfoxide (DMSO), acetone, and other hydrogen bond donor solvents, φ values approach dianionic values [76]. Its sodium salt form finds wide use in angiography [77,78] and glioma studies [79]. Fluorescein 5(6)-isothiocyanate has been used for fluorescence labelling of bacteria, exosomes, proteins (immunofluorescence) and H Protein for gel chromatography. The 5-(iodoacetamido)-fluorescein is used for the synthesis of fluorescently labelled organelles, proteins, peptides and enzymes. Finally, the 5(6)-carboxyfluorescein, a fluorescent polyanionic probe, was used to measure changes in intracellular pH and to highlight processes such as dendrimer aggregation and absorption [80].

3.3 Rhodamine family

These compounds were discovered in 1887. In the 4-10 pH range, their fluorescence spectra are unaffected by changes. The typical chemical structure of rhodamines involves three benzene rings, whose spirocyclic/open-ring conversion results in their off/on fluorescence [81]. In nonpolar solvents, they exist as spirolactone form with very low φ due to disruption of p-conjugation of the xanthene core. In polar solutions, the lactone form undergoes charge separation to form a zwitterion [67]. In open-loop forms, rhodamine dyes exist as ammonium cations that can be driven into mitochondria via MMP (Matrix MetalloProteinase). A famous example is rhodamine 123, which forms the basis of the Mito-Tracker dye [82]. Lastly, the rhodamine 6G is a rhodamine analogue useful in Pgp (P-glycoprotein) efflux assays, and it has been used to characterize the kinetics of MRP1 (multidrug resistance protein 1)- mediated efflux. An in vivo study of rhodamine B-labeled polymeric nanoparticles was conducted by Bonaccorso et al., to evaluate the distribution in brain areas after intranasal administration of the formulation [83].

3.4 Cyanine family

Cyanine dyes are among the most widely used families of fluorophores. Cyanine 5 (Cy5) has five carbon atoms in the bridge. It becomes reversibly photocommutable between a bright and dark state in the presence of a primary thiol [84]. Cy5 excited by visible light undergoes thiolation with a thiol anion and transforms into a non-fluorescent thiolated Cy5. The thiolated Cy5 returns to the light-emitting dethiolated form simply by UV irradiation [85]. The photophysical properties of organic dyes with rotatable bonds are strongly governed by their internal rotation in the excited state since, rotation can greatly affect molecular conformation and bond conjugation [86]. In the biological field, it finds use in comparative genomic hybridization, transcriptomics in proteomics, and RNA localization [87]. Moreover, DiI is a cyanine-derived dialkylcarbon sensitive to the polarity of the environment. It is weakly fluorescent in water, but highly fluorescent in nonpolar solvents. It is commonly used as a lipophilic marker for fluorescence microscopy in the biological field. DiI molecules penetrate in cell membranes with the 2 long alkyl chains (12 carbons) immersed in the bilayer and the rings parallel to the bilayer surface. The dye emits characteristic bright red fluorescence when its alkyl chains are incorporated into membranes making it particularly useful for tracking in the biological membrane [88]. In the study by Musumeci et al., 1-1′-Dioctadecyl-3,3,3 ′, 3′-tetramethylindotricarbocyanine Iodide dye was used to label polymeric nanoparticles and study their cerebral delivery after intranasal administration [89].

3.5 Nile Red

Nile red is an hydrophobic dye of recent interest in the identification of microplastics [90]. It is widely used in biophysical studies focusing on proteins, lipids, and live cell analysis. Depending on the environment, Nile Red shows different absorption and fluorescence spectra. In particular, in organic solvents or nonpolar environments it shows strong fluorescence that changes depending on the environment, presenting shifts towards blue emission in nonpolar environments [91].

3.6 Curcumin

Curcumin is the main natural polyphenol found in the rhizome of *Curcuma longa* (turmeric) and in others *Curcuma* spp. Its countless benefits in the treatment of inflammatory states, metabolic syndrome, pain and inflammatory-degenerative conditions of the eyes are related to its antioxidant and anti-inflammatory effects [92]. Theoretical studies have predicted that its wide absorption band (410 and 430 nm) is due to the π-π * transition while the maximum absorption between 389 and 419 nm is related to the keto and enol form respectively [66].

3.7 Toluidine Blue O

Toluidine blue (TB) is a thiazine-based metachromatic dye. It has a high affinity for acidic tissue components. This characteristic allows colorimetric identification of DNA- and RNA-rich tissues [93]. In ocular field, Navahi et al. performed a study on the use of TB in the diagnosis of ocular surface squamous neoplasm (OSSN) [94]. In the Su et al. study, *in vivo* antibacterial efficacy of TB-mediated photodynamic therapy on bacterial keratitis by *Staphylococcus aureus* in the rabbit was demonstrated. This provides a new option for the clinical treatment of bacterial keratitis [95].

4. Fluorescent nanosystems in ocular application

The following section is focused on recently investigated fluorescent nanomaterials and nanosystems for ocular applications. The reviewed works have been divided according to the use of such fluorescent nanosystems. Most studies concern the use of probes to assess nanosystems distribution within the ocular tissues. Among the most investigated fluorescent nanosystems there are lipid-based nanocarriers - such as nanostructured lipid carriers (NLCs) and solid lipid nanoparticles (SLNs) -, polymeric nanoparticles and nanocapsules, hybrid nanoparticles, cubosomes, emulsomes, nanoemulsions, niosomes, liposomes, films, nanomicelles and hydrogels. Fluorescence is introduced through the methods commonly used to prepare nanosystems [96,97]. The fluorescent nanosystems are essentially divided in i) probe-loaded, in which the dye or probe is encapsulated into the system mostly during the formulation processes, and ii) labelled/grafted, in which the probe is covalently bound to the surface of the nanosystem (often linked to some matrix component, such as polymers or lipids), always forming an adduct (Figure 3).

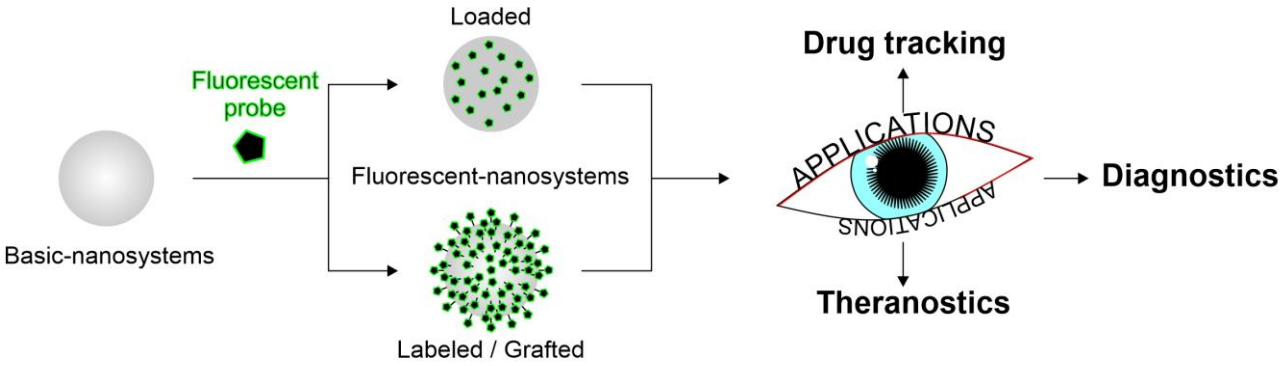

Figure 3. Schematic structure of fluorescent nanosystems for ocular applications.

4.1 Biodistribution

As above cited, the tissues that compose the eye are many and with different properties. The difficulty for a nanosystem to reach the target tissue is high, thus the profile of drug delivery is not always predictable. When the system target is located in deeper ocular tissues, it is even more difficult to predict the ideal pathways followed by the carriers in vivo and through the ocular barriers. Tracking the drug after topical administration is important for several factors. Firstly, it allows to assess the effective achievement of the target site in order to accomplish the desired therapeutic action. Another factor to consider is the non-productive distribution of the drug in non-desired tissues, which could lead to the possible occurrence of side effects besides than reducing the effective drug concentration. Furthermore, studying the pathways followed by the nanosystems is necessary to avoid issues related to barriers, tight junctions and physiological phenomenon (tear flow and blinking) which could impair the routes. Size, surface charge and morphology of the nanocarriers have a great influence on their biodistribution, clearance and cellular uptake [98-101]. Before performing biodistribution studies, it is important to characterize the system and to proceed with *in vitro* and *in vivo* assays. For instance, mean size measurement, zeta potential, mucoadhesion studies, morphological analyses, are of course also required to make the system as conformable as possible to a correct drug release. Tracking of nanosystems can be carried out in two ways, invasive and non-invasive: bioimaging using fluorescent molecules is a non-invasive method [102,103]. Among the most important characteristics that the nanosystem should have there are: small size, necessary to enter cells for allowing bioimaging, high sensitivity for effective detection, fast response, compatibility, absence of toxicity, good dispersibility in the biological environment, highly selective detection in the tissues. In figure 4 a summary is gathered of the fluorescent probes used in the studied nanosystems discussed in sections 4.1, 4.2 and 4.3.

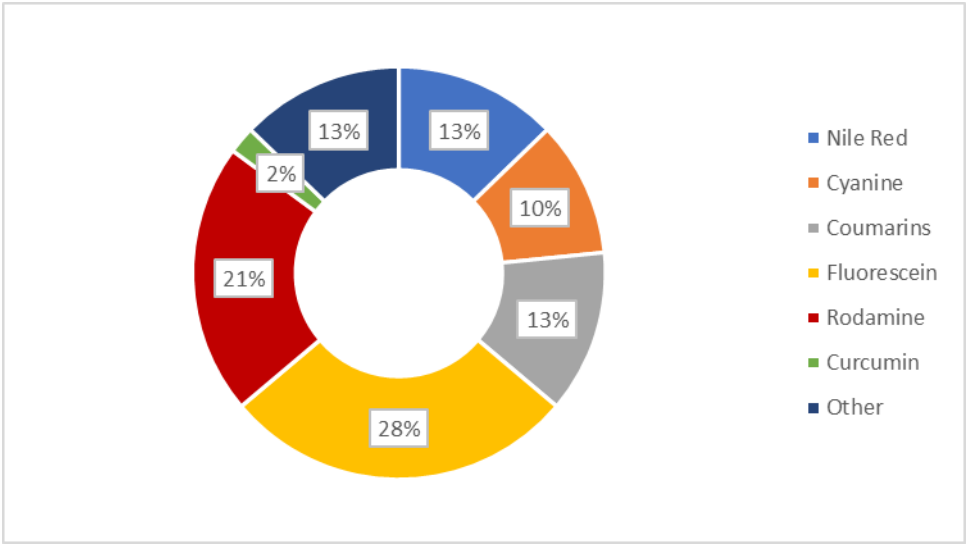

Figure 4. Graphical analysis of the fluorescent probes discussed in this review.

4.1.1 Fluorescent lipid-bases nanosystems

Lipid systems are of great interest for drug delivery in ocular tissues: their biocompatible and biodegradable composition makes them technologically safe, while their lipidic nature and structural characteristics allow them to pass through the corneal layers and achieve an efficient drug dosage even in the deepest tissues of the eye. The distribution of these systems occurs mainly in lipophilic layers, with minimal involvement of the stroma, since it has hydrophilic nature and the lipid systems difficultly distribute there. Due to eye barriers and obstacles for ocular administration, understanding the path taken by the designed nanosystem is necessary, especially if it is targeted to the back of the eye. The main route through which lipid systems reach the deeper tissues is the transcorneal one. There is growing evidence that successful drug delivery by functionalised nanocarriers depends largely on their efficient intra/paracellular transport, a process that is not fully understood yet. Therefore, the development of new imaging and diagnostic techniques is very important, particularly in a complex biological system as the eye. One of the most used dyes for the preparation of fluorescent-lipid nanosystems is Nile Red (NR). In the work of Namprem et al., NLCs were prepared by the high-pressure homogenization method and were labelled using this dye to assess penetration through the cornea. The study, which was conducted using porcine corneas and by confocal scanning microfluorometer (CSMF) analysis, proved the low permeation of NLCs within the stroma [104]. The type of lipid used in the preparation plays an important role in tissue distribution. In the study of El Gendy et al., the same fluorescent probe is used to assess the different permeation provided by cubosomes prepared with different lipid having the role of penetration enhancers. Nanosystems labelled with Nile Red were prepared through emulsification and homogenisation method, comparing the role of nine penetration enhancers: oleic acid, linoleic acid, D-limonene, cineole, Captex® 1000, Captex® 8000, Capmul® MCM, Capmul® PG-8, and Capmul® PG-12. The evaluation was done by CLSM (Confocal laser scanning microscopy) analysis. Among the lipid systems prepared, fluorescence analysis demonstrated that oleic acid, Captex® 8000 and Capmul® MCM played the greatest role in penetration through the corneal layers [105]. Once again, Nile Red was used in the work of Kapadia et al. in order to visualise drug-loaded emulsomes (a novel generation of lipid vesicles), aiming to treat severe inflammation of the eye with corticosteroid triamcinolone acetonide. For the physico-chemical characterisation and subsequent analyses, the nanosystems were prepared with a loaded

drug, while for the studies of precorneal retention and ocular distribution, the fluorescent dye was loaded instead of the drug. The study revealed that after topical administration the pathways taken to reach the back of the eye were basically three: corneal, conjunctival and systemic. The drug can diffuse into the root of the iris and then into the aqueous humour of the posterior chamber and posterior tissues. The drug may diffuse through the sclera by lateral diffusion, followed by penetration of Bruch's membrane and retinal pigment epithelium (RPE). To a lesser extent, the drug may be absorbed into the systemic circulation either through the conjunctival vessels and the nasolacrimal duct, and gain systemic access to the retinal vessel [106]. An in-situ gelling system has been designed for the topical administration of cyclosporine as a potential treatment of dry eye syndrome. The system designed by Eldesouky et al. consisted of lipid nanocapsules (LNC) prepared by phase inversion and temperature cycling methods. To evaluate the distribution of LNC, an *in vivo* fluorescence study was carried out on rabbit cornea. The fluorescence was obtained by labelling LNC with lipophilic dye DiI (1,1-dioctadecyl-3,3,3,3 tetramethyl indocarbocyanine perchlorate). A greater fluorescence was revealed in the corneal epithelium layer than that in the stroma; moreover, a weaker fluorescence was observed for dye dispersion when compared to the dye into LNC, demonstrating that, without the lipid nanocarrier, the dye is not able to cross the hydrophobic corneal layer [107]. With the aim of determining the different distribution of NLCs through the corneal tissues, modified systems decorated with different polymers were designed by Li et al. Firstly, NLCs were prepared with Gelucire 44/14 as a solid lipid, Mygliol 812 as a liquid lipid and Solutol HS15 as a surfactant; subsequently, NLCs were modified with three different types of chitosan: chitosan acetyl-L-cysteine (CS-NAC), chitosan oligosaccharides (COS) and carboxymethyl chitosan (CMCS). Visualisation of the difference in the distribution was carried out by loading the hydrophobic dye C6 into the NLCs. It was revealed through CLSM analysis that NLCs modified with COS and CS-NAC were able to pass through tight junctions, confirming a different influence of the type of coating on the particles transport [108]. Once again, C6 was used to label lipid emulsions of disulfiram. This drug, which inhibits aldehyde dehydrogenase (ALDH1A1), is used for its anti-cataract effect. The addition of octa-arginine (R8) to the nanoemulsions imparted a positive charge to the system, thereby increasing retention in the surface area of the eye. In particular, the permeation of these systems under the influence of particle size and the presence of R8 was investigated. The penetration process of the five preparations (three samples with different sizes, and two of them further modified with R8) through the corneal epithelium was studied, and a three-dimensional reconstruction by CLSM was performed to visualise the distribution of the fluorescent marker within the corneal epithelium. C6 passed through the corneal epithelium mainly by paracellular pathways; moreover, there was also a fluorescent signal in the cytoplasm, indicating that, in addition to paracellular pathways, C6 was also transported by transcellular pathways [109]. As part of the treatment of corneal inflammation, mRNA-based solid lipid nanoparticles were prepared; the fluorescent loaded was Nile Red, used to assess cellular uptake in corneal epithelial cells (HCE-2 cells). The dye was incorporated into the preparation in different ways, depending on the preparation method used to produce the three SLN systems. It was always solubilised in the organic dichloromethane phase, and added either directly at the start, during the first few seconds of sonication or during the re-melting phase. From the uptake studies, it was hypothesised that endocytosis was the route of internalisation into the cells, which is the preferred way exploited by these vectors. This platform could also be used as a theranostic model as GFP (green fluorescent protein) is produced inside the cells, so the intensity of the fluorescence is indicative of the amount of protein produced. Since GFP, once produced, remains at the intracellular level, instillation on the ocular surface of mice of the samples permitted the identification of the corneal layers where transfection occurred. All the prepared mRNA-based SLN formulations showed higher fluorescence intensity than naked mRNA, demonstrating the enhancement of their targeting ability [110]. Fluo-

rescein was used by Jounaki et al. for tracking vancomycin loaded NLCs, basing on the idea that NLCs for topical use could be a valid substitute of intravitreal injection in the treatment of bacterial endophthalmitis promoted especially by *Staphylococcus*. Both drug-loaded and fluorescein-loaded NLCs (0.2mg/ml) were prepared by cold homogenization technique and were used to evaluate precorneal retention with an inverted fluorescent microscope. Sections of dye-loaded NLC-treated eyes presented higher intensities of fluorescent signals in the corneal epithelium, demonstrating that dye-loaded NLCs with a cationic surface (due to the addition of stearylamine) could be trapped and retained in the negatively charged mucin layer covering the ocular surface, facilitating corneal penetration and delivery of the encapsulated compound to intraocular tissues [100]. In the work of Kakkar et al., fluorescein was also used in concentrations almost like the previous work (0.25mg/ml) to track hybrid nanoparticles. Solid lipid nanoparticles were prepared and then coated with PEG, in order to encapsulate the antimycotic fluconazole. Analysis to assess the penetration into the ocular internal layers revealed that fluorescence was observed in the vitreous humour, retina, sclera and choroid after instillation of a single drop of F-SLNs into the rat eye. The particles flowed through the vitreous humour, crossed the inner limiting membrane and reached the outer layers of the retina. In addition, the *ex vivo* study showed that the system exhibited a 164.64% higher flux through the porcine cornea when compared to the commercial drops ZoconVR [111]. The work of Puglia et al. showed different biodistribution of fluorescein-nanoparticles through a more diagnostic *in vivo* study. An adduct is prepared between fluorescein and stearic acid named ODAF (N-(30,60-dihydroxy-3-oxospiro[isobenzofuran-1(3H),90-[9H] xanthen]-5-yl]-octadecanamide). In this platform the dye was grafted (and not loaded) and the conjugation of the lipid with the dye leads to a fluorescent probe. Solvent-diffusion technique was used to prepare SLNs of about 120 nm. The *in vivo* distribution from 1 h to 16 h was evaluated in rabbits and the results showed that, after ocular instillation, ODAF SLNs were mostly located in the cornea (up to 2 h), whereas over a longer time (from the second hour to the eighth hour) the fluorescent signal gradually extended towards the back of the eye [65]. Considering that the influence of blinking and tearing on ocular drug absorption was rarely evaluated in studies, Pretor et al. evaluated absorption using two lipid-based formulations, a liposome and a SLN. The SLNs were also labelled with a fluorescent phospholipid, thus constituting another example of grafted nanosystem. From the study, using C6 as the fluorescent compound, liposomes showed to provide a greater absorption, and the influence of blinking (shear stress of 0.1 Pa.) and tear flow did not affect absorption in these systems. This interesting study, which was conducted to mimic two of the factors underlying ocular physiological mechanisms, was carried out by coupling the use of microfluidics with channels and cultured HCE-T cells as well as the use of a fluorescent dye; it could be very useful to add this kind of assay to the basic characterization of nanosystem addressed to ocular targets [112]. Rhodamine-labelled NLCs were used to assess the corneal retention of such lipid nanocarriers, modified with a complex containing boronic acid, which is able to bind with high affinity the sialic acids of mucin. The NLCs were loaded with dexamethasone and designed for the treatment of dry eye syndrome. Fluorescence marking revealed the increased retention time due to the mucoadhesive property of the nanosystem, which also proved to be a potential not irritant treatment for dry eye syndrome [113]. Another study focused on the preparation of lipid systems (niosomes vesicles) and Eudragit nanoparticles for the treatment of eye fungal infections. Encapsulation of fluconazole within these systems resulted to be a good way to increase the bioavailability of the drug compared to free drug. The systems obtained were innovative in terms of formulation as there is a triple step: the drug was first complexed using β-cyclodextrin, then encapsulated into niosomes and the niosomes were finally incorporated into an *in-situ* gelling system made by Poloxamer, HPMC and chitosan. To assess corneal permeation, the lipid particles were labelled with rhodamine B using the same concentration of the drug without the aid of complexation with cyclodex-

trin, and then were compared to labelled polymeric nanoparticles. The fluorescent signal of CLSM analysis increased in intensity when the NPs were incorporated into the hydrogel, whereas the signal of the pure dye was limited to the superficial epithelial layers, suggesting effective permeation of the nanosystems into the inner tissues [114]. Rhodamine B was also used to study the transport of curcumin as a model drug in multilamellar liposomes. These were coated with sodium alginate grafted acrylic acid conjugated with riboflavin. These multi-dye vesicles (rhodamine and curcumin), prepared using the lipid film hydration technique, have proven to be excellent carriers for drug delivery to the retina. The study evaluated both the encapsulation efficiency of the two dyes and their *in vitro* release. The release test in pH 7.4 medium demonstrated time-depended release, which was faster for rhodamine than for curcumin. Using fluorescence, red for rhodamine and green for curcumin, an extended-release profile was obtained showing greater entrance into the cell at 12 h than at 3 h, and greater endocytosis for smaller, more spherical particles [115].

4.1.2 Polymer-based nanocarriers

Topical delivery of polymeric nanosystems is useful to improve corneal penetration and to prolong the therapeutic response of several drugs. To find clinical application, nanocarriers need to be evaluated in terms of their distribution in biological environment, in order to understand the most appropriate strategy to address specific ocular pathologies. Plausible routes of topically instilled drug delivery for the treatment of ocular diseases involving the posterior segment include several pathways, including corneal, non-corneal, and uveal routes. Successful nanocarrier development therefore involves fluorescent labelling useful to investigate mechanisms and biodistribution profiles of the designed systems. Polymeric nanostructures to be used as imaging diagnostic agents include various kinds of systems, such as nanoparticles, niosomes, film and nanomicelles and in-situ gel. The review of Swetledge et al. offers a detailed discussion on the biodistribution of polymer nanoparticles in major ocular tissues [116]. poly-lactide (PLA), polyglycolide (PGA), poly-lactide-co-glycolide (PLGA), chitosan, Eudragit®, but also different copolymers such as PLGA-PEG, poly-(3-hydroxybutyrate-co-3-hydroxyvalerate) (PHBV) constituted by hydroxybutyrate (HB) and hydroxyvalerate (HV), and chitosan modified copolymer. Depending on the type of polymer, the most suitable fluorescent probe should be chosen. A study conducted by Zhukova et al. was focused on understanding the interactions between probes, polymeric nanoparticles, and biological environment. Four dyes with different degree of hydrophobicity were encapsulated (C6, rhodamine 123, DiI) or covalently bound to the polymer (amine Cyanin 5.5, Cy5.5), in order to label PLGA nanoparticles. To increase the accuracy of the interpretation of biodistribution data, *in vivo* studies after intravenous injection to rats were performed with dual-labelled nanoparticles, using C6 as the encapsulated label and Cy5.5 as the grafted label. A confirmation of the different distribution profile of encapsulated or grafted dyes was obtained from neuroimaging results. The signal of the nanoparticles bounded with Cy5.5 was detected in retinal vessels, whereas the signal of the encapsulated C6 was found outside of blood vessels and in tissue background. The extra vasal distribution of C6 could falsify the data interpretation, making wrongly assume that the nanoparticles could efficiently cross the blood-retinal barrier. Assessing the affinity of the dye to the polymer and the lipophilic structures could be useful in scaling up these issues. Although c6 has not proved to be an ideal label, it aided to explain the phenomenon whereby drugs are delivered to tissues through encapsulation in nanocarriers, without involving the any nanoparticle penetration [117]. Similar results were obtained by Zhang et al. while tracking *in vivo* the distribution of PLGA-NPs in the retinal blood circulation. NPs were labelled with lipophilic perchlorate carbocyanins (DiI) or hydrophilic rhodamine 123 (Rho123). Tracking of fluorescent markers in the rat retina after intravenous injection was performed *in vivo* by real-time imaging and *ex vivo* by microscopy.

DiI fluorescent signal was detected for a long time (> 90 minutes) in retinal vessels, in contrast with Rho123 whose fluorescence was short (> 15 minutes), suggesting diffusion from particles and elimination from the blood circulation: again, the affinity of the dye for the polymer and cell membranes played a key role in biodistribution kinetics. To distinguish between released and encapsulated dye in *in vivo* neuroimaging, dual-labelled nanoparticles were injected intravenously in rats. Colocalization of fluorescent markers was performed by conjugating the polymer with Cy5.5 and loading the systems with probes (DiI/Rho 123). Cy5.5 signal was detected for both cargoes in retinal vessels for mor than 90 minutes, but colocalization was observed only for DiI, indicating that the lipophilic dye was retained within the NPs, while hydrophilic Rho 123 was not detected [118]. Rhodamine B was also loaded into chitosan films designed for the topical treatment of glaucoma. *Ex vivo* permeation studies on rabbit cornea, performed using Franz diffusion cell system, demonstrated the mucoadhesive efficacy of polymeric films in transporting dye molecules through the cornea with a high permeation rate [119]. Rhodamine B isothiocyanate, another derivative of rhodamine family, was used to label polymeric PHBV nanoparticles to obtain information regarding the depth and rate of penetration after topical administration. Confocal analysis performed *ex vivo* on bovine corneas showed that the systems improved the depth of marker penetration into the cornea compared with free RhB used as a control. Topical instillation successfully promoted corneal absorption, making the systems excellent candidates for improving the bioavailability of poorly available drugs [120]. Recently, C6 has also been used as a model drug and a fluorescent marker to track surface-modified PLGA-NPs with chitosan, glycol chitosan, and polysorbate 80 in retinal tissues after topical instillation. Tracking of C6-loaded NPs after eye drops administration in mouse eyes was performed by fluorescence microscopy. The obtained images revealed intense staining throughout the whole eyeball, anterior segment including cornea and conjunctiva, lens, iris/ciliary body, and retina, with a peak at 30 minutes after administration and the disappearance of the signal after 60 minutes. Ocular tissue autofluorescence was distinct around the outer segments of photoreceptor. Based on the average size of the NPs (< 200 nm), the specific pathway of the NPs to the retina did not exclude any of the plausible routes of delivery to the posterior segment after topical instillation (corneal, noncorneal, or uveal pathways) [121]. C6 was also used to label polymeric nanomicelles designed for the topical treatment of fungal keratitis. The nanomicelles consisted of a chitosan oligosaccharide-vitamin E copolymer conjugated to phenylboronic acid (PBA-CS-VE) to enhance corneal retention. C6 delivery through a monolayer of HCE-T cells and 3D cell spheroids demonstrated strong corneal penetration ability. Several characteristics of the polymer were able to influence nanomicelle uptake, but the key role in the process of cellular endocytosis was attributed to the high-affinity interaction between the PBA portion and sialic acid on the surface of the cell membrane [122]. Another study using C6 as a fluorescent probe was reported by Sai et al., aiming to evaluate the corneal transportation of an *in-situ* gelling system based on mixed micelles. This formulation designed for ophthalmic delivery of the polyphenol curcumin was composed of micelles, consisting of 1,2-distearoyl-sn-glycero-3-phosphoethanolamine-N-[methoxy(polyethylene glycol)-2000] (PEG-DSPE) and polyoxyethylene esters of 12-hydroxystearic acid (Solutol HS 15), incorporated in a gellan gum gel. Human corneal epithelial cells (HCEC) were incubated with the fluorescently labelled systems to assess absorption and a greater fluorescence was obtained when the dye was encapsulated into the systems, compared to free C6. In addition, an increase in fluorescence was observed as a function of time, reaching a maximum after 60 minutes. To investigate transcorneal penetration behaviour, *in vivo* permeation studies in rabbits were performed by CLSM using free C6, labelled mixed micelles and gel-incorporated micelles. The designed systems suggested that curcumin is able penetrate more effectively when incorporated into the gelled systems, probably due to the increased retention time conferred by the gellan gum, which was five-fold higher than the mixed micelles alone [123]. A pilot study with C6 was performed to evaluate

the feasibility of the approach in assessing the biodistribution of PLGA-PEG nanoparticles suspended in hydrogels. The preliminary study showed an important limitation due to the high green autofluorescence of the examined ocular tissues. To deal with the drawbacks highlighted by the pilot study, PLGA nanoparticles used in the full study were labelled with Cy-5, a far-red fluorophore that did not overlap with the natural autofluorescence of the ocular tissues. Results from the full study showed that topical application allowed the nanoparticles to be distributed into the outer ocular tissues (cornea, episcleral tissue, and sclera). The choroid was the only internal tissue to show increased fluorescence, although it was lower compared with that of external tissues. It was hypothesized that the nanoparticles detected in the choroid permeated the sclera by absorption of the episcleral tissue, thus avoiding tearing elimination. No fluorescence was detected in retinal tissues, indicating that the NPs were unable to penetrate the blood–retinal barrier (BRB) after topical application [116]. Fluorescein sodium is a dye recently employed as a model drug to label mucoadhesive films based on chitosan and poly(2-ethyl-2-oxazoline) for topical application. To avoid precipitation of complexes formed between the negatively charged dye and the positively charged chitosan backbones, concentrations < 0.1 mg/ml were used. Films tested by *ex vivo* (bovine cornea) and *in vivo* (chinchilla rabbits) studies showed excellent corneal adhesion, with film persisting on the ocular surface for up to 50 minutes [124]. From this review of recently published papers, it emerged that, to ascertain the applicability of nanosystems to biodistribution studies, it is necessary to (i) take into account the degree of affinity and interference between probe, polymeric carriers and cell membranes, and (ii) accurately interpret the data by selecting an effective labelling method upstream. The most reliable way to track the pathways of the systems remains the conjugation of the fluorescent dye to the polymeric core. Therefore, colocalization by double labelling may be the most appropriate technique to minimize errors in the interpretation of fluorescence signals. Currently, there is no unique approach to fluorescent polymer nanosystems that can be used for all types of labelling systems and probes.

4.1.3 Metallic-based and inorganic-based nanosystems

Inorganic nanodevices became of great interest in ocular delivery due to their unique properties such as low cost, easy preparation methods, small size, tuneable porosity, high surface-volume, and robust stability. Fluorescent labelling has been applied to these delivery systems to assess their ability to cross ocular barriers and provide therapeutic efficacy [125]. Corneal barrier functions were investigated by Mun et al. using two types of silica nanoparticles (thiolate and PEGylated) fluorescently labelled with 5-(iodoacetamido)-fluorescein (5-IAF). Permeation studies were performed *in vitro* on intact or β-cyclodextrin pretreated bovine corneas. To provide experimental parameters close to *in vivo* conditions and to avoid artifacts such as the potential risk of corneal swelling when using Franz diffusion cells, the "whole-eye" method was used. 5-IAF-loaded thiolate silica nanoparticles, PEG-grafted silica nanoparticles (5-IAF-PEG), sodium fluorescein and fluorescein isothiocyanate dextran solutions were tested. It resulted that fluorescein salt (376 Da) not uniformly penetrated the cornea; however, the dye was detected in the stroma. Larger molecules such as FITC-dextran (400 Da) and 5-IAF-PEG formed a layer on the corneal surface with no permeation of the epithelial membrane. B-cyclodextrin pre-treatment disrupted the integrity of the cornea by providing homogeneous permeation of the low-molecular-weight dye, although it did not improve penetration of larger molecules. Concerning NPs, no permeation was reported regardless of surface modification, particle size and pre-treatment with β-cyclodextrin, thus suggesting that the tight junctions of the corneal epithelium acted as the main barrier to permeation. Absence of penetration and confinement on the corneal surface were observed for thiolated NPs because of the formation of disulfide bonds between the NPs thiol groups and the cysteine domains of the mucus glycoprotein layer. The interaction between mu-

cin and -SH thiol groups remained a limiting permeation factor even after removal of the epithelial layer. NPs PEGylation was able to mask thiol groups, allowing passage into the stroma [126]. Baran-Rachwalska et al. designed a novel platform consisting of hybrid silicon-lipid nanoparticles, aiming to deliver siRNA to the cornea by topical administration. A fluorescent oligonucleotide duplex, siRNA transfection indicator (siGLO), was employed as a tracking probe to assess *in vitro* cellular uptake on a human corneal epithelial cell line (HCE-S) and *in vivo* corneal penetration on wild-type mice. Red fluorescence of the oligonucleotide marker allowed detection of nanoparticles in all layers of the cornea 3 hours after instillation, in contrast to the control SiGLO. The tracking of biodegradable nanosystems in corneal tissues was confirmed by the reduction of protein expression in the corneal epithelium, making them ideal candidates for therapeutic oligonucleotide delivery [127]. Biodegradable mesoporous silica nanoparticles (MSNs) loaded with carboplatin were designed by Qu et al. for the treatment of retinoblastoma. Carboplatin, being an anticancer drug, causes severe side effects; therefore, it is necessary to focus the action strictly toward the target site. For this purpose, MSNs were surface modified by conjugation with an ideal target, epithelial cell adhesion molecule (EpCAM), in order to increase specificity as well as therapeutic efficacy. To assess the targeting efficacy of the designed systems, the authors evaluated the cellular uptake of untargeted and targeted MSNs in retinoblastoma Y79 tumour cells. Rhodamine B and Lysotracker Green were used as fluorescent probes to track cellular and subcellular uptake of the vectors. Increased cellular uptake for targeted MSNs was attributed to EpCAM-specific receptor-mediated cellular internalization. Lysosomal localization of MSNs confirmed that the nanosystems followed the endocytosis pathway for drug delivery [128]. A hexa-histidine with metal ions nanosystem was designed to deliver Avastin in the treatment of corneal neovascularization (CNV). Pre-corneal retention time and ability to cross ocular barriers were studied on a rat CNV model induced by alkaline burns by FITC labelling the systems. Avastin encapsulated in the vectors showed a longer precorneal adhesion time compared to the free drug. These innovative systems have emerged as a promising platform for ocular topical delivery of protein drugs [129]. An interesting zirconium-porphyrin metal-organic framework (NPMOF) has been designed for drug tracking and delivery. The bright fluorescence self-emitted by the metal-organic framework qualifies the carriers to be applied for imaging. NPMOF was used as a skeleton for the delivery of methylprednisolone, a very efficacious corticosteroid in the treatment of retinal degenerative diseases. Adult zebrafish with photoreceptor degeneration induced by high-intensity light exposure was used to test *in vivo* distribution and therapeutic efficacy. Red fluorescence signals were detected in choroid, retina, photoreceptors, and retinal pigment epithelium for up to 7 days. Recovery of visual function by rapid regeneration of photoreceptors and proliferation of Müller's glia and retinal regeneration were reached after a single intravitreal injection. NPMOF vectors represent a novel delivery systems for the treatment of diseases affecting the posterior eye segment [130].

4.1.4 Protein-based nanosystems

Protein-based nanosystems have attracted considerable interest in recent years and are designed for drug delivery, diagnostics and bioimaging. These highly bio-compatible systems, which have been extensively studied in the biomedical field, owe their properties to the protein they are composed of. Among the proteins used in their preparation, there are antibodies, enzymes, animal and plant proteins, collagen, plasma proteins, gelatin and proteins derived from virus capsids [131]. Fluorescent proteins are usually used to monitor protein-protein interactions, protein localisation and gene expression. However, without any carrier, the fluorescent efficiency of a single protein is relatively low. The use of fluorescent protein-labelled nanomaterials improves loading, due to increased surface area, and allows the development of fluorescent nanosystems useful in

bioimaging and biosensing. In the study carried on by Yang et al., nanoparticles were prepared from regenerated silk fibroin. This protein, which is the most abundant in silk, is considered to have high biocompatibility and degradability properties. In the biomedical field it has been used for drug delivery in small nanosystems, biological drug delivery, gene therapy, wound healing and bone regeneration. The formulation is targeted for intravitreal injection with the aim of increasing the bioavailability of the drug in the retina. Fluorescein isothiocyanate labelled bovine serum albumin (FITC-BSA) has been encapsulated as a model drug. *In vitro* cytotoxicity studies were conducted on ARPE-19 cells, showing that these nanosystems are very compatible. In addition, *in vivo* comparison of the biodistribution in posterior ocular tissues in rabbits revealed an increased retention in the retina due to encapsulation in the nanosystem, rather than with a solution of model drug [132,133]. Albumin is widely used in the preparation of ocular nanosystems [134]. In a recent study, bovine serum albumin nanoparticles loaded with apatinib were prepared for the treatment of diabetic retinopathy. In contrast to the previous study, in this disease invasive administration has to be avoided, so topical administration is the ultimate goal. The nanoparticles were coated with hyaluronic acid (HA) to increase mucoadhesion. The biodistortion study in retinal tissue was carried out by preparing fluorescent nanosystems with 1,1'-dioctadecyl-3,3,3',3'-tetramethylindodicarbocyanine, 4-chlorobenzenesulfonate salt (DiD) solution in ethanol (0.5 mg/mL), which was added during the formulation phase. Through the comparative *in vivo* biodistribution study, it was shown that HA-coated nanoparticles demonstrate higher fluorescence in retinal tissue, compared to uncoated nanoparticles, and thus representing a viable alternative to intravitreal injection, maintaining comparable perfusion and bioavailability [135]. Another study involved the preparation of nanoparticles using pseudo proteins for the potential treatment of ophthalmic diseases. Ten types of nanoparticles obtained by precipitation of pseudo-proteins were prepared, then they were loaded and some of them were also pegylated; finally, they were labelled with a fluorescent probe, fluorescein diacetate (FDA) or rhodamine 6G (Rh6G), to assess ocular penetration. Corneal fluorescence was obtained as expected, while surprising results were the reaching of tissues such as sclera and retina. Thus, they proved to be a promising delivery system for topical use in chronic eye diseases [136].

4.2 Diagnostics

Labelling nanoparticles with fluorescent probes was demonstrated to be a useful approach to improve the effectiveness of some diagnostic tests aimed to early detect ocular pathologies. In fact, some eye diseases require a prompt diagnosis in order to contain possible damages related to the ongoing of the pathways involved. Age-related macular degeneration (AMD) is the main cause of vision lost for over-65-years-old [36]; this pathology has often been analyzed to improve diagnostic techniques, since it has several predisposing factors and an early detection is crucial to avoid degeneration toward blindness [137]. AMD has an unclear etiology, although oxidative stress is considered one of the main risk factors [138]; as a matter of fact, clinical studies demonstrated the importance of supplementation with antioxidants in order to slow down the progression of AMD [139,140]. Physiological antioxidant patterns involve metallothioneins (MT), low molecular mass proteins characterized by the presence of cysteine sulfur ligands, which are able to scavenge free radicals, thus protecting cells and tissues. Retina is particularly subject to oxidative stress due to visible and UV light exposure; moreover, age progression involves a reduction of MT expression, predisposing to AMD [141]. For this reason, bioimaging these proteins in ocular tissues could be an important tool useful to highlight the tendency to develop AMD. For this purpose, fluorescent gold nanoclusters, involving Cu and Zn and bioconjugated with specific primary antibodies, were developed by Cruz-Alonso and coworkers [142]. Laser ablation (LA)-inductively coupled plasma (ICP)-mass spectrometry (MS) technique was used to identify $^{63}Cu^{+}$ and $^{64}Zn^{+}$ in

the retina of post mortem donors, since MT bind both Cu and Zn [143]. This method showed results comparable with conventional immunohistochemistry for MT proteins, with an amplification of signals related to the presence of nanoclusters, which allowed the obtainment of higher resolution bioimages. An *in vivo* model of human "wet" AMD is laser-induced choroidal neovascularization (mouse LCNV) mouse, in which the inflammatory biomarker vascular cell adhesion molecule-1 (VCAM-1) is highly expressed. Aiming to detect this molecule thus assessing the occurrence of oxidative stress, gold nanoparticles functionalized with anti-sense DNA complementary to VCAM-1 mRNA were developed by Uddin et al. [144]. Fluorescence in-situ hybridization (FISH) technique was used to perform photothermal-optical coherence tomography (PT-OCT) involving a fluorescent probe (Alexafluor-647) bonded to 3′ end of anti-sense DNA, in order to highlight its interaction with target mRNA. The conjugation of anti-sense DNA to gold nanoparticles proved to protect from the degradation performed by DNase, while enhancing the uptake, probably through endocytosis, as suggested by transmission electron microscopic (TEM) images of retinal cells; moreover, it was verified that no inference in the fluorescence was produced due to low pH, which is characteristic of inflamed tissues. Comparing to the control group, *in vivo* systemic injection in mice confirmed the enhancement in the fluorescent signal for anti-sense DNA coupled with nanoparticles, which mostly depended on VCAM-1 mRNA hybridization, thus demonstrating the potentiality of the developed platform as a tool to obtain direct images of endogenous mRNA in a tissue. In some cases, this pathology requires transplantation of photoreceptor precursors (PRPs) in the subretinal space, which was successfully performed, guaranteeing a certain vision restoration [145]. Anyway, for a certain period, a monitoring of efficiency of the transplantations needs to be performed. As confirmed by Chemla and coworkers [146], gold nanoparticles could be transplanted together with photoreceptor precursors cells labeled with a fluorescent probe (Alexa 594), in order to ameliorate the efficiency of computed tomography (CT) and optical coherence tomography (OCT) in assessing the success of the transplant. The nanoparticles were firstly characterized in order to assess their safety, thus demonstrating no toxicity toward the transplanted cells and no occurrence of inflammation in retina and vitreous. Furthermore, this platform demonstrated to enhance X-ray signal detected by CT and related to cell survival, without interference from the particles secreted from the cells [147]; moreover, they were also able to increase optical signal for OCT by up to 1.4-fold and to track cells migration toward layers deeper than the injection site. These results confirm the efficiency of such platform in the monitoring of transplantation, but also suggest a potential use for ameliorating existent molecular imaging in cell therapy and diagnostic. Another important diagnostic test is fundus fluorescein angiography (FFA), which allows to highlight vascular leakages in retinal and choroidal pathologies [148]. This clinical tool is useful to diagnose several ocular diseases: age-related macular degeneration, which is characterized by hemorrhaging and exudation in the retina [137]; diabetic retinopathy, that involves retinal damages related to microvascular modification which are clinically not revealable in the early stages [149]; diabetic macular edema, whose pathophysiology implicates modifications of choroidal and retinal vasculature due to BRB impairment [150]. Furthermore, the aforementioned diseases are characterized by alterations of ocular vessels, and share the consequent compromission of visual activity, if not quickly detected and treated. To perform this analysis, fluorescein sodium (FS) is injected intravenously, diffusing in the blood vessels, thus allowing to observe them through confocal scanning laser ophthalmoscopy system. Despite it being considered relatively safe, nausea and vomiting occur frequently, while severe effects like anaphylaxis are rare. The main drawbacks are the diffusion of FS into normal tissues and cellular absorption, with long retention, which were overcome using nanoparticles. Cai et coworkers [148] developed a high-molecular weight polyethyleneimine (PEI) nanoparticles which demonstrated to successfully couple fluorescein; moreover, *in vitro* studies showed good cytocompatibility, not significant difference in apoptosis rates considering various con-

centration tested, no genotoxicity, no morphological changes or significant difference in endothelial tube formation. Cellular uptake assays, carried on with different concentrations of free FS and FS-NP, confirmed similar rapid uptake by cells, with a concentration-dependent and time-dependent fluorescence of main retinal vessels and microvessels. Furthermore, free FS was longer retained into cells when compared to FS-NP, as highlighted by *in vivo* fluorescence studies, suggesting a potential decrease in FS toxicity. These results confirm the potentiality of this platform as a diagnostic tool to detect retinal vessel; moreover, PEI enhances fluorescein metabolism thus reducing its toxicity. Other polymeric nanoparticles developed as a potential diagnostic tool are composed of copolymerized glycerol mono methacrylate (GMMA), glycidyl methacrylate (GME) and ethylene glycol dimethacrylate (EGDMA), which were functionalized with Vancomycin, Polymyxin B, or Amphotericin B, in order to detect the presence of Gram-positive bacteria, Gram-negative bacteria and fungi through specific bond with the respective antibiotic or antimycotic [151]. The occurrence of such bonds was differently highlighted using fluorescent Vancomycin, and probes such as fluorescein isothiocyanate (FITC) and Calcofluor White. Test conducted on various microbiological strains showed a proportional increase in the fluorescence signal with the increase of number of organisms involved; moreover, the presence of functionalized polymers favored the microorganism bonding. Besides the biocompatibility of this platform, another advantage of this platform is the possibility to be shaped as a contact lens requiring only a 30-minute exposure to efficiently detect the occurrence of infection, thus demonstrating to be a promising approach for an easy diagnosis of corneal infections.

4.3 Nanotheranostics

The recent development of systems that integrate the treatment of diseases with their diagnostics is referred to as theranostics. When the system is in a nanoscale range, it is called nanotheranostics. Figure 5 shows prototypes of nanosystems suitable for theranostic purpose.

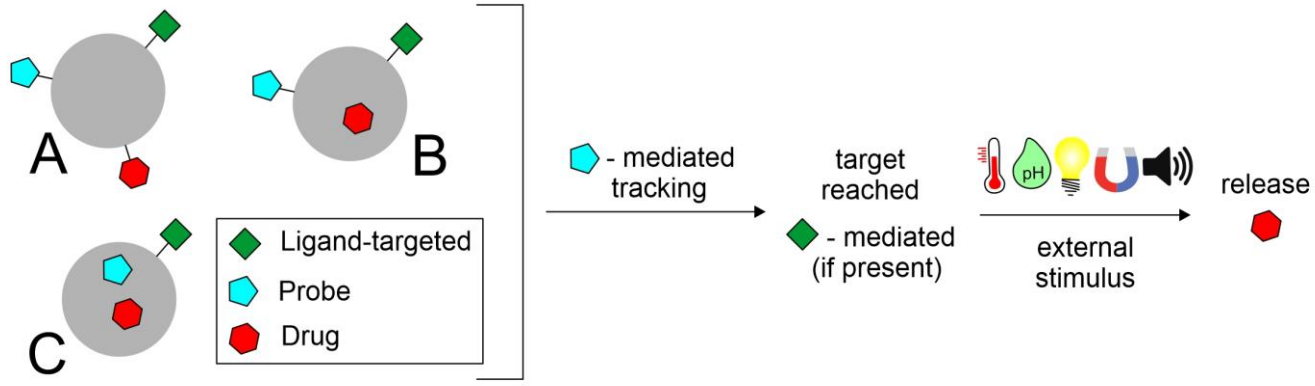

Figure 3. Prototypes of theranostic nanosystems and their mechanism of action. In figure: A) labeling of both probe and drug; B) loading of drug and labeling of probe; C) co-loading of drug and probe.

The development of these applications has given researchers a new way of diagnosing and treating diseases such as cancer, diabetic retinopathy and age-related macular degeneration [36][152]. Among the major chronic eye diseases, diabetic retinopathy is the

most prevalent. Angiogenesis in the posterior eye segment is the main cause of retinal impairment. Clinical management consists of pathological diagnosis and intravitreal injections of vascular endothelial growth factor (VEGF) inhibitors to suppress neovascularisation. The development of innovative nanotheranostic systems is emerging to overcome these critical problems with less invasive methods to synergistically diagnose and treat ocular angiogenesis. Silicon nanoparticles conjugated to the peptide Cyclo-(Arg-Gly-Asp-d-Tyr-Cys) (c-(RGDyC)) (SiNP-RGD) were designed by Tang et al. with the dual action of imaging and treating ocular neovascularization. The effective anti-angiogenic capability of these biocompatible theranostic nanoprobes was based on the combination of a specific detection by labelling endothelial cells and angiogenic blood vessels, and a selective inhibition of neovascularization [153]. Metal NPs are receiving a lot of attention as carriers for the delivery of biomolecules, among which silver NPs (AgNPs) have found numerous applications. Stati et al. designed curcumin stabilized AgNPs using a green and cost-effective method to exploit the promising characteristics of this polyphenol in the *in vivo* treatment of human pterygo. Curcumin is a molecule suitable for theranostic application as widely reported in the work of Shabbir et al., [154]. Pterygo is a progressive eye disease that could culminate in irreversible impairment of visual function. Available treatments require invasive surgical procedures, such as excision, which often leads to a worsening of the clinical picture. Spectroscopic techniques revealed a strong plasmonic resonance between the silver nuclei and the curcumin molecule, demonstrating the presence of the polyphenol on the surface of AgNPs. The biological efficacy of the formulation was tested *in vitro* on human keratinocytes derived from pterygium explants, showing decreased cell viability in treated samples compared to controls. Although no studies have been conducted to track the fate of NPs, the fluorescent emission of the samples could be exploited for bioimaging applications. [155]. Fluorescent silicon nanoparticles modified with Vancomycin were designed by Zhang et al. for the simultaneous non-invasive diagnosis and treatment of keratitis induced by Gram-positive bacteria. These nanotheranostic agents have demonstrated, in combination with a strong antimicrobial activity against *Staphylococcus aureus*, a rapid (< 10 minutes) imaging capability both *in vitro* and *in vivo*. The rapidity with which bacterial keratitis was diagnosed at an early stage suggests that these devices may be useful in preventing the progress of the disease, which could impair visual function if not treated [156]. Oliveira et al. designed hybrid theranostic systems consisting of a lipid matrix of 1,2-dipalmitoyl-sn-glycero-3-phosphatidylcholine (DPPC), coated with Pluronic® F127, covalently bound with the fluorescent probe 5(6)-carboxyfluorescein and loaded with the photosensitising agent verteporfin. Preliminary studies on a glioblastoma cell line (T98G) were conducted to evaluate the potential application as theranostic nanodevices. The fluorescence of the systems revealed on the cancer cell membrane and the 98% reduction in cell viability of T98G cells encouraged further investigation of such multifunctional platforms for the treatment and diagnosis of ophthalmic diseases [157]. Photothermal therapy has been making inroads into the eye sector for a couple of years now. Heat therapy refers to the use of heat as a therapeutic tool to treat diseases such as tumours. In the recent work of Li et al., an approach to treat choroidal melanoma using nanocomposites was designed. Nanosystems were synthesised based on hydrogel, which is itself based on rare-earth nanoparticles. These platforms emit fluorescence in an NIR-II region. Characterised by their tiny size of less than 5 nm, they are targeted to the treatment and simultaneous bioimaging of choroidal melanoma. They have been incorporated into biodegradable hydrogels based on PNIPAM dual response, which could release the drug in a controlled manner by responding to heat and glutathione in the tumour microenvironment. The nanocomposites were then further decorated with indocyanine green (ICS) and folic acid (FA) to enhance therapeutic and targeting specificity and the possibility of achieving photothermal therapy [158]. A lot of studies showed the potential of therapeutic contact lenses in the management of eye disease [159]. Infectious endophthalmitis is a growing concern that causes irreversible damage to intraocular tis-

sue and the optic nerve. The work of Huang et al. focuses on the design of contact lenses consisting of hybrid hydrogels based on quaternized chitosan composite (HTCC), silver nanoparticles and graphene oxide (GO). Fungal keratitis infection often leads to the formation of a biofilm, which is particularly difficult to be penetrated by antifungal agents, especially through eye drops. In addition, the bioavailability of a drug as Voriconazole is very limited. The function of these nanoparticles is not only to deliver Voriconazole in the treatment of fungal keratitis, but also to act as an antimicrobial agent due to its properties. In fact, the materials used, such as quaternized chitosan, have inherent antimicrobial capabilities. The dual functionality makes this system an useful theranostic approach for the treatment of eye infections [160]. The study by Jin et al. reports a therapeutic nanoplatform based on UiO-66-NH_2 to combine photodynamic therapy (PDT) and targeting lipopolysaccharides (LPS) through polypeptide modification (YVLWKRKFCFI-NH_2). The fluorescent used was Toluidine blue (TB), which acts as a photosensitiser (PS) and was loaded into UiO-66-NH_2 nanoparticles (NPs). The dye acts both as a tracer and as a therapeutic agent through photodynamics. The release of the fluorescent is pH dependent. The study proved beneficial against *Pseudomonas aeruginosa* and *Staphylococcus epidermidis* and the *in vivo* model showed positive results in the treatment of endophthalmitis [161].

5. Challenges and future perspectives

The growing number of people suffering from blindness and visual impairment indicates a continuous increase in the need for care and treatment. Given this evidence, urgent action is required to address this largely preventable global problem and provide adequate eye care services. There are still many gaps in literature regarding optimal design and traffic pathways within the eye. In particular, further research is needed to unravel the transport mechanisms across certain barriers in the eye. Moreover, rapid clearance remains a challenge for nanosystems as they need to release their payload before being eliminated from the eye. Many studies focus on assessing the distribution in various tissues once the formulation has been instilled into the eye. Unfortunately, few studies focus on assessing how mechanisms including blinking, tear drainage, and ocular metabolism may interact with nanosystems. Among other things, a very important aspect is the evaluation of the toxicity and the actual applicability of these systems. In fact, many of them are quite complex and the applicability, especially in the theranostic field, is not entirely easy. The evaluation has to be as precise as possible because many eye studies use rodent models; this is highly questionable, especially in the quantification of distribution and kinetic properties of nanoparticles in the eye, as there are many significantly differences between the rodent and human eye. Therefore, the most impactful future studies on this topic will come from larger animal models with eyes that are physiologically and anatomically more similar to ours.

The increasing use of fluorescent probes in the realization of biosensors for colorimetric and radiometric identification of specific targets is a great step forward since the fluorescence represents a non-invasive diagnostic method. This has important benefits in early diagnosis through self-medication screening based on membranes or other platforms containing the appropriate fluorescent probe. These tools are applicable also in epidemics through the realization of specific self-tests based on ELISA or other strategies able to selectively identify the etiological agent. A large and growing field is the use of these probes as part of theranostic photo switch structures, able to change their structure after light stimulus, releasing the therapeutic agent and activating or switching off the fluorescence of the probe. Thus, fluorescence allows accurate and quantitative identification (under certain conditions even by the naked eye as also through *in vitro* tests) of the drug release process. Thus, the use of fluorescent probes is finding increasing use in experimental and advanced ocular chemotherapy using photo-activated systems.

6. Conclusions

The eye has a complex anatomical structure, which represent the main difficulty for drugs to achieve of this target. Nanomedicine has made it possible to overcome several difficulties related to the administration to this almost isolated compartment. The study of the pathways followed by the nanosystems makes it possible to assess the effective achievement of the target site and to consider any non-productive distribution in undesirable tissues with the possible onset of side effects. The biodistribution study also allows the correlation between the chemico-physical parameters of the nanosystems (e.g., ZP, size, morphology, mucoadhesive properties, etc.) and the paths followed by them. This investigation is also aimed at evaluating and developing strategies to bypass physiological barriers of the eye, including tight junctions, tearing and blinking, that could compromise targeting effectiveness. The development of diagnostics mediated by fluorescent probes has improved the efficiency of some diagnostic tests for eye diseases. It is known that early (or rather preventive) diagnosis is a necessity to limit the damage, especially in the long term, caused by specific diseases. This is where the important contribution of fluorescent probes to nanotheranostic approaches becomes relevant, since in these systems diagnostic and therapy coexist. Tracking the nanoparticles makes it possible to highlight the effective achievement of the target, thus follow the release of the therapeutic agent through an external stimulus (e.g., ultrasounds, magnetic fields, light, etc.).

Author Contributions: Conceptualization, R.P.; data curation, C.C. (Cinzia Cimino), S.R., A.R., and E.Z.; writing—original draft preparation, C.C. (Cinzia Cimino), A.R., E.Z.; writing—review and editing, A.B., C.C. (Claudia Carbone), T.M. and R.P.; visualization C.C. (Cinzia Cimino), E.Z.; supervision, R.P.; project administration, R.P.
All coauthors have read and agreed to the present version of the manuscript.

Funding: This research received no external funding.

Institutional Review Board Statement: Not applicable.

Informed Consent Statement: Not applicable.

Data Availability Statement: Not applicable.

Acknowledgments: C. C. (Cinzia Cimino) was supported by the PhD program in Biotechnology, XXXVI cycle, University of Catania; A. R. was supported by the International PhD program in Neurosciences, XXXV cycle, University of Catania and E. Z. was supported by the International PhD program in Neurosciences, XXXVII cycle, University of Catania.

A.B. is a researcher at the University of Catania within the EU-funded PON REACT project (Azione IV.4— "Dottorati e contratti di ricerca su tematiche dell'innovazione", nuovo Asse IV del PON Ricerca e Innovazione 2014–2020 "Istruzione e ricerca per il recupero—REACT—EU"; Progetto "Approcci terapeutici innovativi per il targeting cerebrale di farmaci e materiale genico", CUP E65F21002640005).

Conflicts of Interest: The authors declare no conflict of interest.

References

1. Flaxman, S.R.; Bourne, R.R.A.; Resnikoff, S.; Ackland, P.; Braithwaite, T.; Cicinelli, M. V.; Das, A.; Jonas, J.B.; Keeffe, J.; Kempen, J.; et al. Global causes of blindness and distance vision impairment 1990–2020: a systematic review and meta-analysis. *Lancet Glob. Heal.* **2017**, *5*, e1221–e1234, doi:10.1016/S2214-109X(17)30393-5.
2. Marques, A.P.; Ramke, J.; Cairns, J.; Butt, T.; Zhang, J.H.; Muirhead, D.; Jones, I.; Tong, B.A.M.A.; Swenor, B.K.; Faal, H.; et al. Global economic productivity losses from vision impairment and blindness. *EClinicalMedicine* **2021**, *35*, 100852, doi:10.1016/j.eclinm.2021.100852.
3. Nagarajan, N.; Assi, L.; Varadaraj, V.; Motaghi, M.; Sun, Y.; Couser, E.; Ehrlich, J.R.; Whitson, H.; Swenor, B.K. Vision impairment and cognitive decline among older adults: A systematic review. *BMJ Open* **2022**, *12*, doi:10.1136/bmjopen-2020-047929.
4. Lorenzo-Veiga, B.; Alvarez-Lorenzo, C.; Loftsson, T.; Sigurdsson, H.H. Age-related ocular conditions: Current treatments and role of cyclodextrin-based nanotherapies. *Int. J. Pharm.* **2021**, *603*, 120707, doi:10.1016/j.ijpharm.2021.120707.
5. Pacheco, E.; Lips, M.; Yoong, P. Transition 2.0: Digital technologies, higher education, and vision impairment. *Internet High. Educ.* **2018**, *37*, 1–10, doi:10.1016/j.iheduc.2017.11.001.
6. Bourne, R.R.A.; Steinmetz, J.D.; Saylan, M.; Mersha, A.M.; Weldemariam, A.H.; Wondmeneh, T.G.; Sreeramareddy, C.T.; Pinheiro, M.; Yaseri, M.; Yu, C.; et al. Causes of blindness and vision impairment in 2020 and trends over 30 years, and prevalence of avoidable blindness in relation to VISION 2020: The Right to Sight: An analysis for the Global Burden of Disease Study. *Lancet Glob. Heal.* **2021**, *9*, e144–e160, doi:10.1016/S2214-109X(20)30489-7.
7. Lyu, Q.; Peng, L.; Hong, X.; Fan, T.; Li, J.; Cui, Y.; Zhang, H.; Zhao, J. Smart nano-micro platforms for ophthalmological applications: The state-of-the-art and future perspectives. *Biomaterials* **2021**, *270*, 120682, doi:10.1016/j.biomaterials.2021.120682.
8. Kels, B.D.; Grzybowski, A.; Grant-Kels, J.M. Human ocular anatomy. *Clin. Dermatol.* **2015**, *33*, 140–146, doi:10.1016/j.clindermatol.2014.10.006.
9. Jonas, J.B.; Ohno-Matsui, K.; Panda-Jonas, S. Myopia: Anatomic changes and consequences for its etiology. *Asia-Pacific J. Ophthalmol.* **2019**, *8*, 355–359, doi:10.1097/01.APO.0000578944.25956.8b.
10. Lindfield, D.; Das-Bhaumik, R. Emergency department management of penetrating eye injuries. *Int. Emerg. Nurs.* **2009**, *17*, 155–160, doi:10.1016/j.ienj.2009.01.003.
11. Maulvi, F.A.; Shetty, K.H.; Desai, D.T.; Shah, D.O.; Willcox, M.D.P. Recent advances in ophthalmic preparations: Ocular barriers, dosage forms and routes of administration. *Int. J. Pharm.* **2021**, *608*, 121105, doi:10.1016/j.ijpharm.2021.121105.
12. Suri, R.; Beg, S.; Kohli, K. Target strategies for drug delivery bypassing ocular barriers. *J. Drug Deliv. Sci. Technol.* **2020**, *55*, 101389, doi:10.1016/j.jddst.2019.101389.
13. Varela-Fernández, R.; Díaz-Tomé, V.; Luaces-Rodríguez, A.; Conde-Penedo, A.; García-Otero, X.; Luzardo-álvarez, A.; Fernández-Ferreiro, A.; Otero-Espinar, F.J. Drug delivery to the posterior segment of the eye: Biopharmaceutic and pharmacokinetic considerations. *Pharmaceutics* **2020**, *12*, 1–39, doi:10.3390/pharmaceutics12030269.
14. Madni, A.; Rahem, M.A.; Tahir, N.; Sarfraz, M.; Jabar, A.; Rehman, M.; Kashif, P.M.; Badshah, S.F.; Khan, K.U.; Santos, H.A. Non-invasive strategies for targeting the posterior segment of eye. *Int. J. Pharm.* **2017**, *530*, 326–345, doi:10.1016/j.ijpharm.2017.07.065.
15. Bansal, P.; Garg, S.; Sharma, Y.; Venkatesh, P. Posterior Segment Drug Delivery Devices: Current and Novel Therapies in Development. *J. Ocul. Pharmacol. Ther.* **2016**, *32*, 135–144, doi:10.1089/jop.2015.0133.
16. Kamaleddin, M.A. Nano-ophthalmology: Applications and considerations. *Nanomedicine Nanotechnology, Biol. Med.* **2017**, *13*, 1459–1472, doi:10.1016/j.nano.2017.02.007.
17. Yorston, D. Intravitreal injection technique. *Community Eye Heal. J.* **2014**, *27*, 47, doi:10.5005/jp/books/12170_10.
18. Seah, I.; Zhao, X.; Lin, Q.; Liu, Z.; Su, S.Z.Z.; Yuen, Y. Sen; Hunziker, W.; Lingam, G.; Loh, X.J.; Su, X. Use of biomaterials for sustained delivery of anti-VEGF to treat retinal diseases. *Eye* **2020**, *34*, 1341–1356, doi:10.1038/s41433-020-0770-y

19. Jumelle, C., Gholizadeh, S., Annabi, N., & Dana, R. Advances and limitations of drug delivery systems formulated as eye drops. Journal of *Controlled Release*, **2020**, 321, 1-22.doi:10.1016/j.jconrel.2020.01.057.Advances
20. Shiels, A.; Hejtmancik, J.F. Biology of Inherited Cataracts and Opportunities for Treatment. *Annu. Rev. Vis. Sci.* **2019**, *5*, 123–149, doi:10.1146/annurev-vision-091517-034346.
21. Al-Ghananeem, A.M.; Crooks, P.A. Phase I and phase II ocular metabolic activities and the role of metabolism in ophthalmic prodrug and codrug design and delivery. *Molecules* **2007**, *12*, 373–388, doi:10.3390/12030373.
22. Tang, Z.; Fan, X.; Chen, Y.; Gu, P. Ocular Nanomedicine. *Adv. Sci.* **2022**, *2003699*, 1–36, doi:10.1002/advs.202003699.
23. Leonardi, A.; Bucolo, C.; Drago, F.; Salomone, S.; Pignatello, R. Cationic solid lipid nanoparticles enhance ocular hypotensive effect of melatonin in rabbit. *Int. J. Pharm.* **2015**, *478*, 180–186, doi:10.1016/j.ijpharm.2014.11.032.
24. Burhan, A.M.; Klahan, B.; Cummins, W.; Andrés-Guerrero, V.; Byrne, M.E.; O'reilly, N.J.; Chauhan, A.; Fitzhenry, L.; Hughes, H. Posterior segment ophthalmic drug delivery: Role of muco-adhesion with a special focus on chitosan. *Pharmaceutics* **2021**, *13*, doi:10.3390/pharmaceutics13101685.
25. Gautam, D.; Pedler, M.G.; Nair, D.P.; Petrash, J.M. Nanogel-facilitated in-situ delivery of a cataract inhibitor. *Biomolecules* **2021**, *11*, 1–12, doi:10.3390/biom11081150.
26. Gagandeep; Garg, T.; Malik, B.; Rath, G.; Goyal, A.K. Development and characterization of nano-fiber patch for the treatment of glaucoma. *Eur. J. Pharm. Sci.* **2014**, *53*, 10–16, doi:10.1016/j.ejps.2013.11.016.
27. Ghosh, A.K.; Thapa, R.; Hariani, H.N.; Volyanyuk, M.; Ogle, S.D.; Orloff, K.A.; Ankireddy, S.; Lai, K.; Žiniauskaitė, A.; Stubbs, E.B.; et al. Poly(Lactic-co-glycolic acid) nanoparticles encapsulating the prenylated flavonoid, xanthohumol, protect corneal epithelial cells from dry eye disease-associated oxidative stress. *Pharmaceutics* **2021**, *13*, doi:10.3390/pharmaceutics13091362.
28. Shi, L.; Li, Z.; Liang, Z.; Zhang, J.; Liu, R.; Chu, D.; Han, L.; Zhu, L.; Shen, J.; Li, J. A dual-functional chitosan derivative platform for fungal keratitis. *Carbohydr. Polym.* **2022**, *275*, 118762, doi:10.1016/j.carbpol.2021.118762.
29. Liu, Y.C.; Lin, M.T.Y.; Ng, A.H.C.; Wong, T.T.; Mehta, J.S. Nanotechnology for the treatment of allergic conjunctival diseases. *Pharmaceuticals* **2020**, *13*, 1–21, doi:10.3390/ph13110351.
30. Nirbhavane, P.; Sharma, G.; Singh, B.; Begum, G.; Jones, M.C.; Rauz, S.; Vincent, R.; Denniston, A.K.; Hill, L.J.; Katare, O.P. Triamcinolone acetonide loaded-cationic nano-lipoidal formulation for uveitis: Evidences of improved biopharmaceutical performance and anti-inflammatory activity. *Colloids Surfaces B Biointerfaces* **2020**, *190*, 110902, doi:10.1016/j.colsurfb.2020.110902.
31. Du, S.; Wang, H.; Jiang, F.; Wang, Y. Diabetic Retinopathy Analysis—Effects of Nanoparticle-Based Triamcinolone. *J. Nanosci. Nanotechnol.* **2020**, *20*, 6111–6115, doi:10.1166/jnn.2020.18569.
32. Suri, R.; Neupane, Y.R.; Mehra, N.; Nematullah, M.; Khan, F.; Alam, O.; Iqubal, A.; Jain, G.K.; Kohli, K. Sirolimus loaded chitosan functionalized poly (lactic-co-glycolic acid) (PLGA) nanoparticles for potential treatment of age-related macular degeneration. *Int. J. Biol. Macromol.* **2021**, *191*, 548–559, doi:10.1016/j.ijbiomac.2021.09.069.
33. Youssef, A.; Dudhipala, N.; Majumdar, S. Pharmaceutics-12-00572. **2020**, 1–19.
34. Tabatabaei, S.N.; Derbali, R.M.; Yang, C.; Superstein, R.; Hamel, P.; Chain, J.L.; Hardy, P. Co-delivery of miR-181a and melphalan by lipid nanoparticles for treatment of seeded retinoblastoma. *J. Control. Release* **2019**, *298*, 177–185, doi:10.1016/j.jconrel.2019.02.014.
35. Allyn, M.M.; Luo, R.H.; Hellwarth, E.B.; Swindle-Reilly, K.E. Considerations for Polymers Used in Ocular Drug Delivery. *Front. Med.* **2022**, *8*, 1–25, doi:10.3389/fmed.2021.787644.
36. Divya, K.; Yashwant V., P.; Kevin B., S. Theranostic Applications of Nanomaterials for Ophthalmic Applications. *Int. J. Sci. Adv.* **2021**, *2*, 354–364, doi:10.51542/ijscia.v2i3.20.
37. Awwad, S.; Mohamed Ahmed, A.H.A.; Sharma, G.; Heng, J.S.; Khaw, P.T.; Brocchini, S.; Lockwood, A. Principles of pharmacology in the eye. *Br. J. Pharmacol.* **2017**, *174*, 4205–4223, doi:10.1111/bph.14024.
38. Dosmar, E.; Walsh, J.; Doyel, M.; Bussett, K.; Oladipupo, A.; Amer, S.; Goebel, K. Targeting Ocular Drug Delivery: An Examination of Local Anatomy and Current Approaches. *Bioengineering* **2022**, *9*, doi:10.3390/bioengineering9010041.
39. Atta, G.; Tempfer, H.; Kaser-Eichberger, A.; Traweger, A.; Heindl, L.M.; Schroedl, F. Is the human sclera a tendon-like tissue? A structural and functional comparison. *Ann. Anat.* **2022**, *240*, 151858, doi:10.1016/j.aanat.2021.151858.

40. Lopes, B.T.; Bao, F.; Wang, J.; Liu, X.; Wang, L.; Abass, A.; Eliasy, A.; Elsheikh, A. Review of in-vivo characterisation of corneal biomechanics. *Med. Nov. Technol. Devices* **2021**, *11*, 100073, doi:10.1016/j.medntd.2021.100073.
41. Zénon, A. Eye pupil signals information gain. *Proc. R. Soc. B Biol. Sci.* **2019**, *286*, 0–1, doi:10.1098/rspb.2019.1593.
42. Domkin, D.; Forsman, M.; Richter, H.O. Effect of ciliary-muscle contraction force on trapezius muscle activity during computer mouse work. *Eur. J. Appl. Physiol.* **2019**, *119*, 389–397, doi:10.1007/s00421-018-4031-8.
43. Chow, L.S.; Paley, M.N.J. Recent advances on optic nerve magnetic resonance imaging and post-processing. *Magn. Reson. Imaging* **2021**, *79*, 76–84, doi:10.1016/j.mri.2021.03.014.
44. Kaur, I.P.; Smitha, R.; Aggarwal, D.; Kapil, M. Acetazolamide: Future perspective in topical glaucoma therapeutics. *Int. J. Pharm.* **2002**, *248*, 1–14, doi:10.1016/S0378-5173(02)00438-6.
45. Nielsen, L.H.; Keller, S.S.; Boisen, A. Microfabricated devices for oral drug delivery. *Lab Chip* **2018**, *18*, 2348–2358, doi:10.1039/c8lc00408k.
46. Underhill, G.H.; Khetani, S.R. Advances in engineered human liver platforms for drug metabolism studies. *Drug Metab. Dispos.* **2018**, *46*, 1626–1637, doi:10.1124/dmd.118.083295.
47. Pitkänen, L.; Ranta, V.P.; Moilanen, H.; Urtti, A. Permeability of retinal pigment epithelium: Effects of permeant molecular weight and lipophilicity. *Investig. Ophthalmol. Vis. Sci.* **2005**, *46*, 641–646, doi:10.1167/iovs.04-1051.
48. Reinholz, J.; Landfester, K.; Mailänder, V. The challenges of oral drug delivery via nanocarriers. *Drug Deliv.* **2018**, *25*, 1694–1705, doi:10.1080/10717544.2018.1501119.
49. Kim, Y.C.; Chiang, B.; Wu, X.; Prausnitz, M.R. Ocular delivery of macromolecules. *J. Control. Release* **2014**, *190*, 172–181, doi:10.1016/j.jconrel.2014.06.043.
50. Urtti, A. Challenges and obstacles of ocular pharmacokinetics and drug delivery. *Adv. Drug Deliv. Rev.* **2006**, *58*, 1131–1135, doi:10.1016/j.addr.2006.07.027.
51. Falavarjani, K.G.; Nguyen, Q.D. Adverse events and complications associated with intravitreal injection of anti-VEGF agents: A review of literature. *Eye* **2013**, *27*, 787–794, doi:10.1038/eye.2013.107.
52. Ibrahim, S.S. The Role of Surface Active Agents in Ophthalmic Drug Delivery: A Comprehensive Review. *J. Pharm. Sci.* **2019**, *108*, 1923–1933, doi:10.1016/j.xphs.2019.01.016.
53. Liebmann, J.M.; Barton, K.; Weinreb, R.N.; Eichenbaum, D.A.; Gupta, P.K.; McCabe, C.M.; Wolfe, J.D.; Ahmed, I.; Sheybani, A.; Craven, E.R. Evolving Guidelines for Intracameral Injection. *J. Glaucoma* **2020**, *29*, 1–7, doi:10.1097/IJG.0000000000001451.
54. Takahashi, K.; Morizane, Y.; Hisatomi, T.; Tachibana, T.; Kimura, S.; Hosokawa, M.M.; Shiode, Y.; Hirano, M.; Doi, S.; Toshima, S.; et al. The influence of subretinal injection pressure on the microstructure of the monkey retina. *PLoS One* **2018**, *13*, 1–15, doi:10.1371/journal.pone.0209996.
55. Sebbag, L.; Moody, L.M.; Mochel, J.P. Albumin levels in tear film modulate the bioavailability of medically-relevant topical drugs. *Front. Pharmacol.* **2020**, *10*, 1–9, doi:10.3389/fphar.2019.01560.
56. Järvinen, K.; Järvinen, T.; Urtti, A. Ocular absorption following topical delivery. *Adv. Drug Deliv. Rev.* **1995**, *16*, 3–19, doi:10.1016/0169-409X(95)00010-5.
57. Patere, S.; Newman, B.; Wang, Y.; Choi, S.; Vora, S.; Ma, A.W.K.; Jay, M.; Lu, X. Influence of Manufacturing Process Variables on the Properties of Ophthalmic Ointments of Tobramycin. *Pharm. Res.* **2018**, *35*, doi:10.1007/s11095-018-2462-x.
58. Lazcano-Gomez, G.; Castillejos, A.; Kahook, M.; Jimenez-Roman, J.; Gonzalez-Salinas, R. Videographic assessment of glaucoma drop instillation. *J. Curr. Glaucoma Pract.* **2015**, *9*, 47–50, doi:10.5005/jp-journals-10008-1183.
59. Taneja, M.; Chappidi, K.; Harsha Ch, S.N.S.; Richhariya, A.; Mohamed, A.; Rathi, V.M. Innovative bulls eye drop applicator for self-instillation of eye drops. *Contact Lens Anterior Eye* **2020**, *43*, 256–260, doi:10.1016/j.clae.2019.11.010.
60. Davies, I.; Williams, A.M.; Muir, K.W. Aids for eye drop administration. *Surv. Ophthalmol.* **2017**, *62*, 332–345, doi:10.1016/j.survophthal.2016.12.009.
61. Hornof, M.; Toropainen, E.; Urtti, A. Cell culture models of the ocular barriers. *Eur. J. Pharm. Biopharm.* **2005**, *60*, 207–225, doi:10.1016/j.ejpb.2005.01.009.
62. Juretić, M.; Cetina-Čižmek, B.; Filipović-Grčić, J.; Hafner, A.; Lovrić, J.; Pepić, I. Biopharmaceutical evaluation of surface active ophthalmic excipients using in vitro and ex vivo corneal models. *Eur. J. Pharm. Sci.* **2018**, *120*, 133–141, doi:10.1016/j.ejps.2018.04.032.

63. Li, Q.; Weng, J.; Wong, S.N.; Thomas Lee, W.Y.; Chow, S.F. Nanoparticulate Drug Delivery to the Retina. *Mol. Pharm.* **2021**, *18*, 506–521, doi:10.1021/acs.molpharmaceut.0c00224.
64. Karki, R.; Meena, M.; Prakash, T.; Rajeswari, T.; Goli, D.; Kumar, S. Reduction in drop size of ophthalmic topical drop preparations and the impact of treatment. *J. Adv. Pharm. Technol. Res.* **2011**, *2*, 192, doi:10.4103/2231-4040.85540.
65. Puglia, C.; Santonocito, D.; Romeo, G.; Intagliata, S.; Romano, G.L.; Strettoi, E.; Novelli, E.; Ostacolo, C.; Campiglia, P.; Sommella, E.M.; et al. Lipid nanoparticles traverse non-corneal path to reach the posterior eye segment: In vivo evidence. *Molecules* **2021**, *26*, 1–11, doi:10.3390/molecules26154673.
66. Bechnak, L.; El Kurdi, R.; Patra, D. Fluorescence Sensing of Nucleic Acid by Curcumin Encapsulated Poly(Ethylene Oxide)-Block-Poly(Propylene Oxide)-Block-Poly(Ethylene Oxide) Based Nanocapsules. *J. Fluoresc.* **2020**, *30*, 547–556, doi:10.1007/s10895-020-02528-9.
67. Beija, M.; Afonso, C.A.M.; Martinho, J.M.G. Synthesis and applications of rhodamine derivatives as fluorescent probes. *Chem. Soc. Rev.* **2009**, *38*, 2410–2433, doi:10.1039/b901612k.
68. Han, Z.X.; Zhang, X.B.; Li, Z.; Gong, Y.J.; Wu, X.Y.; Jin, Z.; He, C.M.; Jian, L.X.; Zhang, J.; Shen, G.L.; et al. Efficient fluorescence resonance energy transfer-based ratiometric fluorescent cellular imaging probe for Zn2+ using a rhodamine spirolactam as a trigger. *Anal. Chem.* **2010**, *82*, 3108–3113, doi:10.1021/ac100376a.
69. Keerthana, S.; Sam, B.; George, L.; Sudhakar, Y.N.; Varghese, A. Fluorescein Based Fluorescence Sensors for the Selective Sensing of Various Analytes. *J. Fluoresc.* **2021**, *31*, 1251–1276, doi:10.1007/s10895-021-02770-9.
70. El Khoury, E.; Patra, D. Length of hydrocarbon chain influences location of curcumin in liposomes: Curcumin as a molecular probe to study ethanol induced interdigitation of liposomes. *J. Photochem. Photobiol. B Biol.* **2016**, *158*, 49–54, doi:10.1016/j.jphotobiol.2016.02.022.
71. Khorasani, M.Y.; Langari, H.; Sany, S.B.T.; Rezayi, M.; Sahebkar, A. The role of curcumin and its derivatives in sensory applications. *Mater. Sci. Eng. C* **2019**, *103*, 109792, doi:10.1016/j.msec.2019.109792.
72. Carneiro, A.; Matos, M.J.; Uriarte, E.; Santana, L. Trending topics on coumarin and its derivatives in 2020. *Molecules* **2021**, *26*, 1–15, doi:10.3390/molecules26020501.
73. Duong, H.D.; Shin, Y.; Rhee, J. Il Development of novel optical pH sensors based on coumarin 6 and nile blue A encapsulated in resin particles and specific support materials. *Mater. Sci. Eng. C* **2020**, *107*, 110323, doi:10.1016/j.msec.2019.110323.
74. Grimm, J.B.; Lavis, L.D. Synthesis of rhodamines from fluoresceins using pd-catalyzed c-n cross-coupling. *Org. Lett.* **2011**, *13*, 6354–6357, doi:10.1021/ol202618t.
75. Rajasekar, M. Recent development in fluorescein derivatives. *J. Mol. Struct.* **2021**, *1224*, 129085, doi:10.1016/j.molstruc.2020.129085.
76. McHedlov-Petrossyan, N.O.; Cheipesh, T.A.; Roshal, A.D.; Shekhovtsov, S. V.; Moskaeva, E.G.; Omelchenko, I. V. Aminofluoresceins Versus Fluorescein: Peculiarity of Fluorescence. *J. Phys. Chem. A* **2019**, *123*, 8860–8870, doi:10.1021/acs.jpca.9b05812.
77. Zhao, X.; Belykh, E.; Cavallo, C.; Valli, D.; Gandhi, S.; Preul, M.C.; Vajkoczy, P.; Lawton, M.T.; Nakaji, P. Application of Fluorescein Fluorescence in Vascular Neurosurgery. *Front. Surg.* **2019**, *6*, doi:10.3389/fsurg.2019.00052.
78. Küçükyürük, B.; Korkmaz, T.Ş.; Nemayire, K.; Özlen, F.; Kafadar, A.M.; Akar, Z.; Kaynar, M.Y.; Sanus, G.Z. Intraoperative Fluorescein Sodium Videoangiography in Intracranial Aneurysm Surgery. *World Neurosurg.* **2021**, *147*, e444–e452, doi:10.1016/j.wneu.2020.12.085.
79. Bömers, J.P.; Danielsen, M.E.; Schulz, M.K.; Halle, B.; Kristensen, B.W.; Sørensen, M.D.; Poulsen, F.R.; Pedersen, C.B. Sodium fluorescein shows high surgeon-reported usability in glioblastoma surgery. *Surgeon* **2020**, *18*, 344–348, doi:10.1016/j.surge.2020.01.003.
80. Voronin, D. V.; Kozlova, A.A.; Verkhovskii, R.A.; Ermakov, A. V.; Makarkin, M.A.; Inozemtseva, O.A.; Bratashov, D.N. Detection of rare objects by flow cytometry: Imaging, cell sorting, and deep learning approaches. *Int. J. Mol. Sci.* **2020**, *21*, doi:10.3390/ijms21072323.
81. Wang, L.; Du, W.; Hu, Z.; Uvdal, K.; Li, L.; Huang, W. Hybrid Rhodamine Fluorophores in the Visible/NIR Region for Biological Imaging. *Angew. Chemie - Int. Ed.* **2019**, *58*, 14026–14043, doi:10.1002/anie.201901061.
82. Marnett, L.J. Synthesis of 5- and 6-Carboxy-X-rhodamines. **2008**, 2007–2009.

83. Bonaccorso, A.; Musumeci, T.; Serapide, M.F.; Pellitteri, R.; Uchegbu, I.F.; Puglisi, G. Nose to brain delivery in rats: Effect of surface charge of rhodamine B labeled nanocarriers on brain subregion localization. *Colloids Surfaces B Biointerfaces* **2017**, *154*, 297–306, doi:10.1016/j.colsurfb.2017.03.035.
84. Dempsey, G.T.; Bates, M.; Kowtoniuk, W.E.; Liu, D.R.; Tsien, R.Y.; Zhuang, X. Photoswitching mechanism of cyanine dyes. *J. Am. Chem. Soc.* **2009**, *131*, 18192–18193, doi:10.1021/ja904588g.
85. Lim, E.; Kwon, J.; Park, J.; Heo, J.; Kim, S.K. Selective thiolation and photoswitching mechanism of Cy5 studied by time-dependent density functional theory. *Phys. Chem. Chem. Phys.* **2020**, *22*, 14125–14129, doi:10.1039/d0cp00026d.
86. Bae, S.; Lim, E.; Hwang, D.; Huh, H.; Kim, S.K. Torsion-dependent fluorescence switching of amyloid-binding dye NIAD-4. *Chem. Phys. Lett.* **2015**, *633*, 109–113, doi:10.1016/j.cplett.2015.05.010.
87. Blower, M.D.; Feric, E.; Weis, K.; Heald, R. Genome-wide analysis demonstrates conserved localization of messenger RNAs to mitotic microtubules. *J. Cell Biol.* **2007**, *179*, 1365–1373, doi:10.1083/jcb.200705163.
88. Martos, A.; Berger, M.; Kranz, W.; Spanopoulou, A.; Menzen, T.; Friess, W.; Wuchner, K.; Hawe, A. Novel High-Throughput Assay for Polysorbate Quantification in Biopharmaceutical Products by Using the Fluorescent Dye DiI. *J. Pharm. Sci.* **2020**, *109*, 646–655, doi:10.1016/j.xphs.2019.10.013.
89. Musumeci, T.; Serapide, M.F.; Pellitteri, R.; Dalpiaz, A.; Ferraro, L.; Dal Magro, R.; Bonaccorso, A.; Carbone, C.; Veiga, F.; Sancini, G.; et al. Oxcarbazepine free or loaded PLGA nanoparticles as effective intranasal approach to control epileptic seizures in rodents. *Eur. J. Pharm. Biopharm.* **2018**, *133*, 309–320, doi:10.1016/j.ejpb.2018.11.002.
90. Capolungo, C.; Genovese, D.; Montalti, M.; Rampazzo, E.; Zaccheroni, N.; Prodi, L. Photoluminescence-Based Techniques for the Detection of Micro- and Nanoplastics. *Chem. - A Eur. J.* **2021**, *27*, 17529–17541, doi:10.1002/chem.202102692.
91. Sancataldo, G.; Avellone, G.; Vetri, V. Nile Red lifetime reveals microplastic identity. *Environ. Sci. Process. Impacts* **2020**, *22*, 2266–2275, doi:10.1039/d0em00348d.
92. Hewlings, S.J.; Kalman, D.S. Curcumin: A review of its effects on human health. *Foods* **2017**, *6*, 1–11, doi:10.3390/foods6100092.
93. Sridharan, G.; Shankar, A.A. Toluidine blue: A review of its chemistry and clinical utility. *J. Oral Maxillofac. Pathol.* **2012**, *16*, 251–255, doi:10.4103/0973-029X.99081.
94. Aliakbar Navahi, R.; Hosseini, S.B.; Kanavi, M.R.; Rakhshani, N.; Aghaei, H.; Kheiri, B. Comparison of toluidine blue 1% staining patterns in cytopathologically confirmed ocular surface squamous neoplasias and in non-neoplastic lesions. *Ocul. Surf.* **2019**, *17*, 578–583, doi:10.1016/j.jtos.2019.04.010.
95. Su, G.; Wei, Z.; Wang, L.; Shen, J.; Baudouin, C.; Labbé, A.; Liang, Q. Evaluation of toluidine blue-mediated photodynamic therapy for experimental bacterial keratitis in rabbits. *Transl. Vis. Sci. Technol.* **2020**, *9*, 1–10, doi:10.1167/tvst.9.3.13.
96. Craparo, E.F.; Musumeci, T.; Bonaccorso, A.; Pellitteri, R.; Romeo, A.; Naletova, I.; Cucci, L.M.; Cavallaro, G.; Satriano, C. Mpeg-plga nanoparticles labelled with loaded or conjugated rhodamine-b for potential nose-to-brain delivery. *Pharmaceutics* **2021**, *13*, doi:10.3390/pharmaceutics13091508.
97. Turcsányi, Á.; Ungor, D.; Csapó, E. Fluorescent labeling of hyaluronic acid-chitosan nanocarriers by protein-stabilized gold nanoclusters. *Crystals* **2020**, *10*, 1–15, doi:10.3390/cryst10121113.
98. Romero, G.B.; Keck, C.M.; Müller, R.H.; Bou-Chacra, N.A. Development of cationic nanocrystals for ocular delivery. *Eur. J. Pharm. Biopharm.* **2016**, *107*, 215–222, doi:10.1016/j.ejpb.2016.07.005.
99. Pignatello, R.; Corsaro, R.; Santonocito, D. Chapter A Method for Efficient Loading of Ciprofloxacin Hydrochloride in Cationic Solid Lipid Nanoparticles. **2019**, 2–31.
100. Jounaki, K.; Makhmalzadeh, B.S.; Feghhi, M.; Heidarian, A. Topical ocular delivery of vancomycin loaded cationic lipid nanocarriers as a promising and non-invasive alternative approach to intravitreal injection for enhanced bacterial endophthalmitis management. *Eur. J. Pharm. Sci.* **2021**, *167*, 105991, doi:10.1016/j.ejps.2021.105991.
101. Vaishya, R.D.; Khurana, V.; Patel, S.; Mitra, A.K. Controlled ocular drug delivery with nanomicelles. *Wiley Interdiscip. Rev. Nanomedicine Nanobiotechnology* **2014**, *6*, 422–437, doi:10.1002/wnan.1272.
102. Siddique, S.; Chow, J.C.L. Application of nanomaterials in biomedical imaging and cancer therapy. *Nanomaterials* **2020**, *10*, 1–41, doi:10.3390/nano10091700.
103. Zhang, W.H.; Hu, X.X.; Zhang, X.B. Dye-doped fluorescent silica nanoparticles for live cell and in vivo bioimaging. *Nanomaterials* **2016**, *6*, doi:10.3390/nano6050081.

104. Niamprem, P.; Srinivas, S.P.; Tiyaboonchai, W. Penetration of Nile red-loaded nanostructured lipid carriers (NLCs) across the porcine cornea. *Colloids Surfaces B Biointerfaces* **2019**, *176*, 371–378, doi:10.1016/j.colsurfb.2019.01.018.
105. El-Gendy, M.A.; Mansour, M.; El-Assal, M.I.A.; Ishak, R.A.H.; Mortada, N.D. Delineating penetration enhancer-enriched liquid crystalline nanostructures as novel platforms for improved ophthalmic delivery. *Int. J. Pharm.* **2020**, *582*, 119313, doi:10.1016/j.ijpharm.2020.119313.
106. Kapadia, R.; Parikh, K.; Jain, M.; Sawant, K. Topical instillation of triamcinolone acetonide-loaded emulsomes for posterior ocular delivery: statistical optimization and in vitro-in vivo studies. *Drug Deliv. Transl. Res.* **2021**, *11*, 984–999, doi:10.1007/s13346-020-00810-8.
107. Eldesouky, L.M.; El-Moslemany, R.M.; Ramadan, A.A.; Morsi, M.H.; Khalafallah, N.M. Cyclosporine lipid nanocapsules as thermoresponsive gel for dry eye management: Promising corneal mucoadhesion, biodistribution and preclinical efficacy in rabbits. *Pharmaceutics* **2021**, *13*, doi:10.3390/pharmaceutics13030360.
108. Li, J.; Tan, G.; Cheng, B.; Liu, D.; Pan, W. Transport mechanism of chitosan-N-acetylcysteine, chitosan oligosaccharides or carboxymethyl chitosan decorated coumarin-6 loaded nanostructured lipid carriers across the rabbit ocular. *Eur. J. Pharm. Biopharm.* **2017**, *120*, 89–97, doi:10.1016/j.ejpb.2017.08.013.
109. Liu, C.; Lan, Q.; He, W.; Nie, C.; Zhang, C.; Xu, T.; Jiang, T.; Wang, S. Octa-arginine modified lipid emulsions as a potential ocular delivery system for disulfiram: A study of the corneal permeation, transcorneal mechanism and anti-cataract effect. *Colloids Surfaces B Biointerfaces* **2017**, *160*, 305–314, doi:10.1016/j.colsurfb.2017.08.037.
110. Gómez-Aguado, I.; Rodríguez-Castejón, J.; Beraza-Millor, M.; Vicente-Pascual, M.; Rodríguez-Gascón, A.; Garelli, S.; Battaglia, L.; Del Pozo-Rodríguez, A.; Solinís, M.Á. Mrna-based nanomedicinal products to address corneal inflammation by interleukin-10 supplementation. *Pharmaceutics* **2021**, *13*, doi:10.3390/pharmaceutics13091472.
111. Kakkar, S.; Singh, M.; Mohan Karuppayil, S.; Raut, J.S.; Giansanti, F.; Papucci, L.; Schiavone, N.; Nag, T.C.; Gao, N.; Yu, F.S.X.; et al. Lipo-PEG nano-ocular formulation successfully encapsulates hydrophilic fluconazole and traverses corneal and non-corneal path to reach posterior eye segment. *J. Drug Target.* **2021**, *29*, 631–650, doi:10.1080/1061186X.2020.1871483.
112. Pretor, S.; Bartels, J.; Lorenz, T.; Dahl, K.; Finke, J.H.; Peterat, G.; Krull, R.; Dietzel, A.; Bu, S.; Behrends, S.; et al. Cellular Uptake of Coumarin - 6 under Micro fl uidic Conditions into HCE - T Cells from Nanoscale Formulations. **2014**.
113. Tan, G.; Li, J.; Song, Y.; Yu, Y.; Liu, D.; Pan, W. Phenylboronic acid-tethered chondroitin sulfate-based mucoadhesive nanostructured lipid carriers for the treatment of dry eye syndrome. *Acta Biomater.* **2019**, *99*, 350–362, doi:10.1016/j.actbio.2019.08.035.
114. Elmotasem, H.; Awad, G.E.A. A stepwise optimization strategy to formulate in situ gelling formulations comprising fluconazole-hydroxypropyl-beta-cyclodextrin complex loaded niosomal vesicles and Eudragit nanoparticles for enhanced antifungal activity and prolonged ocular delivery. *Asian J. Pharm. Sci.* **2020**, *15*, 617–636, doi:10.1016/j.ajps.2019.09.003.
115. Anishiya chella daisy, E.R.; Rajendran, N.K.; Jeyaraj, M.; Ramu, A.; Rajan, M. Retinal photoreceptors targeting SA-g-AA coated multilamellar liposomes carrier system for cytotoxicity and cellular uptake evaluation. *J. Liposome Res.* **2021**, *31*, 203–216, doi:10.1080/08982104.2020.1768111.
116. Swetledge, S.; Carter, R.; Stout, R.; Astete, C.E.; Jung, J.P.; Sabliov, C.M. Stability and ocular biodistribution of topically administered PLGA nanoparticles. *Sci. Rep.* **2021**, *11*, 1–11, doi:10.1038/s41598-021-90792-5.
117. Zhukova, V.; Osipova, N.; Semyonkin, A.; Malinovskaya, J.; Melnikov, P.; Valikhov, M.; Porozov, Y.; Solovev, Y.; Kuliaev, P.; Zhang, E.; et al. Fluorescently labeled plga nanoparticles for visualization in vitro and in vivo: The importance of dye properties. *Pharmaceutics* **2021**, *13*, doi:10.3390/pharmaceutics13081145.
118. Zhang, E.; Zhukova, V.; Semyonkin, A.; Osipova, N.; Malinovskaya, Y.; Maksimenko, O.; Chernikov, V.; Sokolov, M.; Grigartzik, L.; Sabel, B.A.; et al. Release kinetics of fluorescent dyes from PLGA nanoparticles in retinal blood vessels: In vivo monitoring and ex vivo localization. *Eur. J. Pharm. Biopharm.* **2020**, *150*, 131–142, doi:10.1016/j.ejpb.2020.03.006.
119. Li, B.; Wang, J.; Gui, Q.; Yang, H. Drug-loaded chitosan film prepared via facile solution casting and air-drying of plain water-based chitosan solution for ocular drug delivery. *Bioact. Mater.* **2020**, *5*, 577–583, doi:10.1016/j.bioactmat.2020.04.013.
120. Álvarez-Álvarez, L.; Barral, L.; Bouza, R.; Farrag, Y.; Otero-Espinar, F.; Feijóo-Bandín, S.; Lago, F. Hydrocortisone loaded poly-(3-hydroxybutyrate-co-3-hydroxyvalerate) nanoparticles for topical ophthalmic

administration: Preparation, characterization and evaluation of ophthalmic toxicity. *Int. J. Pharm.* **2019**, *568*, 118519, doi:10.1016/j.ijpharm.2019.118519.
121. Tahara, K.; Karasawa, K.; Onodera, R.; Takeuchi, H. Feasibility of drug delivery to the eye's posterior segment by topical instillation of PLGA nanoparticles. *Asian J. Pharm. Sci.* **2017**, *12*, 394–399, doi:10.1016/j.ajps.2017.03.002.
122. Sun, X.; Sheng, Y.; Li, K.; Sai, S.; Feng, J.; Li, Y.; Zhang, J.; Han, J.; Tian, B. Mucoadhesive phenylboronic acid conjugated chitosan oligosaccharide-vitamin E copolymer for topical ocular delivery of voriconazole: Synthesis, in vitro/vivo evaluation, and mechanism. *Acta Biomater.* **2022**, *138*, 193–207, doi:10.1016/j.actbio.2021.10.047.
123. Sai, N.; Dong, X.; Huang, P.; You, L.; Yang, C.; Liu, Y.; Wang, W.; Wu, H.; Yu, Y.; Du, Y.; et al. A novel gel-forming solution based on PEG-DSPE/Solutol HS 15 mixed micelles and gellan gum for ophthalmic delivery of curcumin. *Molecules* **2020**, *25*, 1–15, doi:10.3390/molecules25010081.
124. Abilova, G.K.; Kaldybekov, D.B.; Ozhmukhametova, E.K.; Saimova, A.Z.; Kazybayeva, D.S.; Irmukhametova, G.S.; Khutoryanskiy, V. V. Chitosan/poly(2-ethyl-2-oxazoline) films for ocular drug delivery: Formulation, miscibility, in vitro and in vivo studies. *Eur. Polym. J.* **2019**, *116*, 311–320, doi:10.1016/j.eurpolymj.2019.04.016.
125. Chi, H.; Gu, Y.; Xu, T.; Cao, F. Multifunctional organic–inorganic hybrid nanoparticles and nanosheets based on chitosan derivative and layered double hydroxide: Cellular uptake mechanism and application for topical ocular drug delivery. *Int. J. Nanomedicine* **2017**, *12*, 1607–1620, doi:10.2147/IJN.S129311.
126. Mun, E.A.; Morrison, P.W.J.; Williams, A.C.; Khutoryanskiy, V. V. On the barrier properties of the cornea: A microscopy study of the penetration of fluorescently labeled nanoparticles, polymers, and sodium fluorescein. *Mol. Pharm.* **2014**, *11*, 3556–3564, doi:10.1021/mp500332m.
127. Baran-Rachwalska, P.; Torabi-Pour, N.; Sutera, F.M.; Ahmed, M.; Thomas, K.; Nesbit, M.A.; Welsh, M.; Moore, C.B.T.; Saffie-Siebert, S.R. Topical siRNA delivery to the cornea and anterior eye by hybrid silicon-lipid nanoparticles. *J. Control. Release* **2020**, *326*, 192–202, doi:10.1016/j.jconrel.2020.07.004.
128. Qu, W.; Meng, B.; Yu, Y.; Wang, S. EpCAM antibody-conjugated mesoporous silica nanoparticles to enhance the anticancer efficacy of carboplatin in retinoblastoma. *Mater. Sci. Eng. C* **2017**, *76*, 646–651, doi:10.1016/j.msec.2017.03.036.
129. Xu, H.; Tang, B.; Huang, W.; Luo, S.; Zhang, T.; Yuan, J.; Zheng, Q.; Zan, X. Deliver protein across bio-barriers via hexa-histidine metal assemblies for therapy: a case in corneal neovascularization model. *Mater. Today Bio* **2021**, *12*, doi:10.1016/j.mtbio.2021.100143.
130. Wang, Y.; Liu, W.; Yuan, B.; Yin, X.; Li, Y.; Li, Z.; Cui, J.; Yuan, X.; Li, Y. The application of methylprednisolone nanoscale zirconium-porphyrin metal-organic framework (MPS-NPMOF) in the treatment of photoreceptor degeneration. *Int. J. Nanomedicine* **2019**, *14*, 9763–9776, doi:10.2147/IJN.S225992.
131. Ding, S.; Zhang, N.; Lyu, Z.; Zhu, W.; Chang, Y.C.; Hu, X.; Du, D.; Lin, Y. Protein-based nanomaterials and nanosystems for biomedical applications: A review. *Mater. Today* **2021**, *43*, 166–184, doi:10.1016/j.mattod.2020.11.015.
132. Nguyen, T.P.; Nguyen, Q.V.; Nguyen, V.H.; Le, T.H.; Huynh, V.Q.N.; Vo, D.V.N.; Trinh, Q.T.; Kim, S.Y.; Van Le, Q. Silk fibroin-based biomaterials for biomedical applications: A review. *Polymers (Basel).* **2019**, *11*, 1–25, doi:10.3390/polym11121933.
133. Yang, P.; Dong, Y.; Huang, D.; Zhu, C.; Liu, H.; Pan, X.; Wu, C. Silk fibroin nanoparticles for enhanced bio-macromolecule delivery to the retina. *Pharm. Dev. Technol.* **2019**, *24*, 575–583, doi:10.1080/10837450.2018.1545236.
134. Tiwari, R.; Sethiya, N.K.; Gulbake, A.S.; Mehra, N.K.; Murty, U.S.N.; Gulbake, A. A review on albumin as a biomaterial for ocular drug delivery. *Int. J. Biol. Macromol.* **2021**, *191*, 591–599, doi:10.1016/j.ijbiomac.2021.09.112.
135. Radwan, S.E.S.; El-Kamel, A.; Zaki, E.I.; Burgalassi, S.; Zucchetti, E.; El-Moslemany, R.M. Hyaluronic-coated albumin nanoparticles for the non-invasive delivery of apatinib in diabetic retinopathy. *Int. J. Nanomedicine* **2021**, *16*, 4481–4494, doi:10.2147/IJN.S316564.
136. Zhang, W.; Kantaria, T.; Zhang, Y.; Kantaria, T.; Kobauri, S.; Tugushi, D.; Brücher, V.; Katsarava, R.; Eter, N.; Heiduschka, P. Biodegradable Nanoparticles Based on Pseudo-Proteins Show Promise as Carriers for Ophthalmic Drug Delivery. *J. Ocul. Pharmacol. Ther.* **2020**, *36*, 421–432, doi:10.1089/jop.2019.0148.
137. Thomas, C.J.; Mirza, R.G.; Gill, M.K. Age-Related Macular Degeneration. *Med. Clin. North Am.* **2021**, *105*, 473–491, doi:10.1016/j.mcna.2021.01.003.
138. Hanus J, Anderson C, Wang S. RPE necroptosis in response to oxidative stress and in AMD. *Ageing Res Rev.* **2015** doi: 10.1016/j.arr.2015.09.002.

139. Hammond, B.R.; Johnson, M.A. The age-related eye disease study (AREDS). *Nutr. Rev.* **2002**, *60*, 283–288, doi:10.1301/002966402320387215.
140. Gregori, N.Z.; Goldhardt, R. Nutritional Supplements for Age-Related Macular Degeneration. *Curr. Ophthalmol. Rep.* **2015**, *3*, 34–39, doi:10.1007/s40135-014-0059-z.
141. Álvarez-Barrios, A.; Álvarez, L.; García, M.; Artime, E.; Pereiro, R.; González-Iglesias, H. Antioxidant defenses in the human eye: A focus on metallothioneins. *Antioxidants* **2021**, *10*, 1–33, doi:10.3390/antiox10010089.
142. Cruz-Alonso, M.; Fernandez, B.; Álvarez, L.; González-Iglesias, H.; Traub, H.; Jakubowski, N.; Pereiro, R. Bioimaging of metallothioneins in ocular tissue sections by laser ablation-ICP-MS using bioconjugated gold nanoclusters as specific tags. *Microchim. Acta* **2018**, *185*, 1–9, doi:10.1007/s00604-017-2597-1.
143. Osredkar, J. Copper and Zinc, Biological Role and Significance of Copper/Zinc Imbalance. *J. Clin. Toxicol.* **2011**, *s3*, 1–18, doi:10.4172/2161-0495.s3-001.
144. Uddin, M. I., Kilburn, T. C., Yang, R., McCollum, G. W., Wright, D. W., & Penn, J. S.. Targeted imaging of VCAM-1 mRNA in a mouse model of laser-induced choroidal neovascularization using antisense hairpin-DNA-functionalized gold-nanoparticles. *Molecular pharmaceutics* **2018,** 15(12), 5514-5520.
145. Pearson RA, Barber AC, Rizzi M et al. Restoration of vision after transplantation of photoreceptors. *Nature* **2012,** 485(7396), 99–103.
146. Chemla, Y.; Betzer, O.; Markus, A.; Farah, N.; Motiei, M.; Popovtzer, R.; Mandel, Y. Gold nanoparticles for multimodal high-resolution imaging of transplanted cells for retinal replacement therapy. *Nanomedicine* **2019**, *14*, 1857–1871, doi:10.2217/nnm-2018-0299.
147. Meir, R.; Shamalov, K.; Betzer, O.; Motiei, M.; Horovitz-Fried, M.; Yehuda, R.; Popovtzer, A.; Popovtzer, R.; Cohen, C.J. Nanomedicine for Cancer Immunotherapy: Tracking Cancer-Specific T-Cells in Vivo with Gold Nanoparticles and CT Imaging. *ACS Nano* **2015**, *9*, 6363–6372, doi:10.1021/acsnano.5b01939.
148. Cai, W.; Chen, M.; Fan, J.; Jin, H.; Yu, D.; Qiang, S.; Peng, C.; Yu, J. Fluorescein sodium loaded by polyethyleneimine for fundus fluorescein angiography improves adhesion. *Nanomedicine* **2019**, *14*, 2595–2611, doi:10.2217/nnm-2019-0008.
149. Safi, H.; Safi, S.; Hafezi-Moghadam, A.; Ahmadieh, H. Early detection of diabetic retinopathy. *Surv. Ophthalmol.* **2018**, *63*, 601–608, doi:10.1016/j.survophthal.2018.04.003.
150. Wang, X.; Li, S.; Li, W.; Hua, Y.; Wu, Q. Choroidal Variations in Diabetic Macular Edema: Fluorescein Angiography and Optical Coherence Tomography. *Curr. Eye Res.* **2018**, *43*, 102–108, doi:10.1080/02713683.2017.1370115.
151. Shivshetty, N.; Swift, T.; Pinnock, A.; Pownall, D.; Neil, S. Mac; Douglas, I.; Garg, P.; Rimmer, S. Evaluation of ligand modified poly (N-Isopropyl acrylamide) hydrogel for etiological diagnosis of corneal infection. *Exp. Eye Res.* **2022**, *214*, 108881, doi:10.1016/j.exer.2021.108881.
152. Ladju, R.B.; Ulhaq, Z.S.; Soraya, G.V. Nanotheranostics: A powerful next-generation solution to tackle hepatocellular carcinoma. *World J. Gastroenterol.* **2022**, *28*, 176–187, doi:10.3748/wjg.v28.i2.176.
153. Tang, M.; Ji, X.; Xu, H.; Zhang, L.; Jiang, A.; Song, B.; Su, Y.; He, Y. Photostable and Biocompatible Fluorescent Silicon Nanoparticles-Based Theranostic Probes for Simultaneous Imaging and Treatment of Ocular Neovascularization. *Anal. Chem.* **2018**, *90*, 8188–8195, doi:10.1021/acs.analchem.8b01580.
154. Shabbir, U.; Rubab, M.; Tyagi, A.; Oh, D.H. Curcumin and its derivatives as theranostic agents in alzheimer's disease: The implication of nanotechnology. *Int. J. Mol. Sci.* **2021**, *22*, 1–23, doi:10.3390/ijms22010196.
155. Stati, G.; Rossi, F.; Trakoolwilaiwan, T.; Tung, L.D.; Mourdikoudis, S.; Thanh, N.T.K.; Di Pietro, R. Development and Characterization of Curcumin-Silver Nanoparticles as a Promising Formulation to Test on Human Pterygium-Derived Keratinocytes. *Molecules* **2022**, *27*, 1–11, doi:10.3390/molecules27010282.
156. Zhang, L.; Ji, X.; Su, Y.; Zhai, X.; Xu, H.; Song, B.; Jiang, A.; Guo, D.; He, Y. Fluorescent silicon nanoparticles-based nanotheranostic agents for rapid diagnosis and treatment of bacteria-induced keratitis. *Nano Res.* **2021**, *14*, 52–58, doi:10.1007/s12274-020-3039-7.
157. de Oliveira, D.C.S.; de Freitas, C.F.; Calori, I.R.; Goncalves, R.S.; Cardinali, C.A.E.F.; Malacarne, L.C.; Ravanelli, M.I.; de Oliveira, H.P.M.; Tedesco, A.C.; Caetano, W.; et al. Theranostic verteporfin- loaded lipid-polymer liposome for photodynamic applications. *J. Photochem. Photobiol. B Biol.* **2020**, *212*, 112039, doi:10.1016/j.jphotobiol.2020.112039.

158. Li, L.; Zeng, Z.; Chen, Z.; Gao, R.; Pan, L.; Deng, J.; Ye, X.; Zhang, J.; Zhang, S.; Mei, C.; et al. Microenvironment-triggered degradable hydrogel for imaging diagnosis and combined treatment of intraocular choroidal melanoma. *ACS Nano* **2020**, *14*, 15403–15416, doi:10.1021/acsnano.0c06000.
159. Maulvi, F.A.; Desai, D.T.; Shetty, K.H.; Shah, D.O.; Willcox, M.D.P. Advances and challenges in the nanoparticles-laden contact lenses for ocular drug delivery. *Int. J. Pharm.* **2021**, *608*, 121090, doi:10.1016/j.ijpharm.2021.121090.
160. Huang, J.F.; Zhong, J.; Chen, G.P.; Lin, Z.T.; Deng, Y.; Liu, Y.L.; Cao, P.Y.; Wang, B.; Wei, Y.; Wu, T.; et al. A Hydrogel-Based Hybrid Theranostic Contact Lens for Fungal Keratitis. *ACS Nano* **2016**, *10*, 6464–6473, doi:10.1021/acsnano.6b00601.
161. Jin, Y.; Wang, Y.; Yang, J.; Zhang, H.; Yang, Y.W.; Chen, W.; Jiang, W.; Qu, J.; Guo, Y.; Wang, B. An Integrated Theranostic Nanomaterial for Targeted Photodynamic Therapy of Infectious Endophthalmitis. *Cell Reports Phys. Sci.* **2020**, *1*, 100173, doi:10.1016/j.xcrp.2020.100173.